Simulation of the Atlantic Circulation with a Coupled Sea Ice–Mixed Layer–Isopycnal General Circulation Model. Part I: Model Description

JOSEF M. OBERHUBER*

Meteorologisches Institut der Universität Hamburg, Hamburg, Germany

(Manuscript received 8 July 1991, in final form 18 May 1992)

ABSTRACT

A diabatic ocean general circulation model based on primitive equations is described. It uses isopycnals as Lagrangian coordinates in the vertical and predicts a free surface. Prognostic fields of temperature and salinity enter the dynamics as active tracers through a realistic equation of state. The surface boundary layer is parameterized by a detailed mixed-layer model. A sea ice model with a viscous–plastic rheology is coupled to the mixed layer. Thermal forcing, wind stress, and surface input of turbulent kinetic energy are determined from monthly mean values of atmospheric quantities, while the freshwater flux still is parameterized by a Newtonian relaxation towards the observed surface salinity.

The model equations are written in layer formulation. Each interface represents an isopycnal. As the equations are written in flux form, the mass flux and the content of mass, heat, and salt are conserved in the model domain. A potential vorticity conserving scheme is included. Except for the mixed layer, all layers are kept at a prescribed potential density that is different for each layer. In the uppermost layer, potential density is allowed to develop arbitrarily. A method is developed that treats vanishing layers by making the horizontal boundaries time dependent in each layer. The time integration scheme consists of a predictor–corrector technique combined with a semi-implicit scheme. The model is formulated in spherical coordinates with variable, but still orthogonal, grid resolution in longitude and latitude and allows for any irregular geometry.

1. Introduction

Cartesian coordinates are commonly used to formulate fluid mechanical models. Based on these coordinates Bryan (1969) developed the Geophysical Fluid Dynamics Laboratory (GFDL) model, based on primitive equations and formulated on the sphere. It represented a milestone in ocean modeling. By including a realistic equation of state for sea water, it already contained combined temperature and salinity effects. The GFDL model was the first running code capable of simulating the global circulation. Semtner (1974) and Cox (1975, 1984) recoded and improved Bryan's formulation, meanwhile, becoming the most frequently used ocean model worldwide.

Because it uses primitive equations, this concept of a numerical model requires a large amount of computer resources. Therefore, Maier-Reimer and Hasselmann (1987) formulated, in a separate line of development, a highly efficient global model by application of the geostrophic approximation, thus permitting inexpensive integrations modeling thousands of years. The long advective time scales of the deep ocean make this feature necessary for carrying out many tracer experiments.

But Lagrangian coordinates also have many attractive features, especially for the representation of a highly conservative fluid such as the subsurface ocean. They allow particles to conserve advective properties exactly. However, the steady deformation of the grid causes spatial derivatives (e.g., pressure gradients) to become increasingly difficult to estimate with increasing integration time. A compromise that overcomes this difficulty is to choose the coordinate planes in the vertical as space and time dependent in such a way that particles move on these planes if they conserve their property exactly. In the case of the ocean, potential density can be used as coordinate planes. On these planes conventional Cartesian coordinates can be employed to discretize the equations in longitude and latitude. Since the model should be used for large-scale studies only, additional terms in the equations of motion resulting from the curvature of the potential density planes can be neglected.

The choice of these coordinates ensures that the dynamically active part of the diffusion, namely the cross-isopycnal part, is totally excluded if this process is not parameterized explicitly. A rotation of the diffusion operators on to isopycnal coordinates, as proposed by

* Permanent affiliation: Max-Planck-Institut für Meteorologie, Hamburg, Germany.

Corresponding author address: Dr. Josef M. Oberhuber, Max-Planck-Institut für Meteorologie, Bundesstrasse 55, D-2000 Hamburg 13, West Germany.

Redi (1982) and McDougal and Church (1986) for z-coordinate models, is superfluous. Since the transport of heat and salt along an isopycnal has no impact on the potential density and, hence, on the pressure field, errors in the advection discretization have to a first order no influence on the dynamics. Another advantage of isopycnic coordinates is that baroclinic structures require fewer layers in isopycnic coordinates than levels in z coordinates to obtain a similar vertical resolution. Lagrangian coordinates automatically migrate into those regions where fronts are starting to develop. Because the positions of fronts are not known a priori, a level model needs a high resolution at all those locations where a front might occur.

Numerical models with isopycnic coordinates remain simple as long as thermodynamics are not included. If salinity is either kept constant or assumed to have no dynamical impact, only temperature determines the potential density. In this case, it is not necessary to predict temperature and salinity to determine the oceanic pressure field. It is sufficient to specify a horizontally homogeneous stability between two adjacent layers. Such models are used to study the wind-driven circulation but are, of course, not capable of studying combined effects of temperature and salinity as they become increasingly important towards higher latitudes. Many models with such a restriction have been used for studying the ocean. Robinson (1965) was the first to use potential density coordinates. For the atmosphere, Bleck (1974, 1984) and Shapiro (1975) developed models with isentropic coordinates. Such multilayer models have had some success in simulating lee cyclogenesis mainly due to the conservation of potential vorticity. However, an essential part of the atmospheric heating takes place in the free atmosphere through convective rainfall and radiation. Therefore, particles do not conserve their heat content. Since the diabatic heating of the ocean is confined to the surface except for a few narrow areas of deep convection, it is more obvious to use the concept of isopycnal coordinates for the ocean. Bleck and Boudra (1981) presented a model based on isopycnic coordinates. They made some compromise by moving locally to Cartesian coordinates whenever a layer disappeared into the surface or the topography. More recently, Bleck and Boudra (1986) treated the problem of vanishing layers by taking the FCT (flux corrected transport) algorithm of Boris and Book (1973) and Zalesak (1979). Using the same technique, Bogue et al. (1986) and Huang and Bryan (1987) formulated a similar model, but with the inclusion of a surface boundary layer of constant depth, which permitted a crude treatment of thermal forcing.

The motivation for the modeling efforts described in this paper is to fill a gap in the hierarchy of ocean models. A model with isopycnic coordinates has not yet been developed that includes a satisfactory representation of thermodynamics—as in Bryan's model or that of Maier-Reimer and Hasselmann—for vertical mixing and convection that allows an arbitrary geometry. Such a numerical model is developed here and tested by application to the Atlantic circulation (see Part II). Meanwhile, Bleck (personal communication) is also developing a model to include two active tracers.

The paper is structured as follows: section 2 contains the model description. The underlying equations of the ocean model are presented in section 2a, the mixed-layer model in section 2b, the parameterizations of the surface fluxes in section 2c, the treatment of internal diffusion in section 2d, the sea ice formulation in section 2e, and a general description of the numerical techniques in section 2f.

2. Model formulation

Two types of surface boundary conditions enter the description of the upper ocean, namely the ocean–atmosphere fluxes in the open ocean and the influence of sea ice on these fluxes. The momentum flux can be taken from observed fields of stresses. The evaluation of heat fluxes is more critical. They determine the SST directly and indirectly the mixed layer thickness and therefore the response time scale to atmospheric forcing. An ocean model with a prognostic mixed layer responds differently to external forcing from a model with a prescribed boundary-layer thickness. It is therefore important to reduce errors in the model forcing by improving the heat flux computation. This also has to be considered as preparation for coupling the model to an AGCM.

The question arises as to whether it is advisable to allow an outcropping of layers at the surface. The high turbulence activity in the surface boundary layer allows particles to cross isopycnals easily. Thus, it is not meaningful to represent the surface boundary layer with Lagrangian coordinates. A further complication is the technical problem of how to distribute surface fluxes among the several shallow near-surface layers that could occur. Therefore, the uppermost ocean is represented by a separate surface boundary model (see Fig. 1), having the advantage that the thickness of the boundary layer yields a more realistic response time scale to atmospheric forcing. Its vertical structure is idealized by the bulk mixed-layer approach.

Sea ice is a further component of the complete ocean dynamics. Over large areas, it controls exchange processes between atmosphere and ocean and contributes through its own dynamics to the forcing of the ocean. Sea ice has significant influences on the internal stratification near the ocean surface. It is partly responsible for the production of salty, cold and therefore, heavy water that influences the vertical stratification globally.

The representation of the interior ocean by isopycnic layers and the surface layer by a mixed-layer approach leads to the question of how both components must be coupled without violating the constraint to maintain the isopycnal coordinates used for the deep ocean.

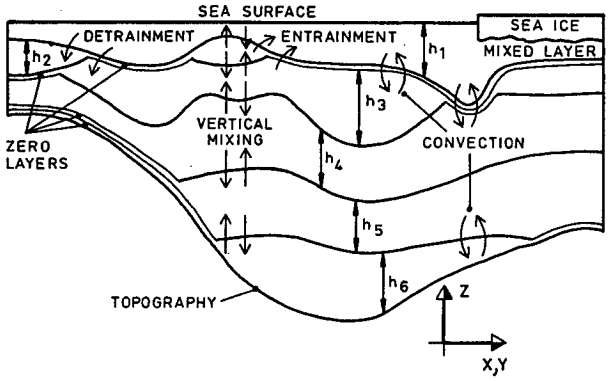

FIG. 1. Vertical cross section of the layer thickness distribution. The mixed layer is the uppermost layer; lower layers are the isopycnic layers. Arrows indicate mass transfer rates representing various mixing parameterizations.

From our understanding of the ocean it is evident that atmospheric information enters the ocean at its surface and propagates essentially along isopycnals into the deep ocean. Schopf (1983), Schopf and Cane (1983), and Schopf and Harrison (1983) developed a technique for coupling a mixed-layer model to an underlying layer model. They obtained some improvement with regard to the propagation of equatorial waves and the SST response during an El Niño over models without a mixed layer. However, further difficulties arise because of the constraint that the potential density of the underlying layer is, by definition, constant in an isopycnal model. Basically the mixed layer and the underlying isopycnal model work with different coordinates (see Fig. 1). As long as entrainment is considered, the potential density in the next deeper layer is unchanged. But in the detrainment case, water with an arbitrary potential density may not be injected into an isopycnic layer with an a priori specified potential density. Potential density conservation would be violated. This is a conceptual problem to be explained later.

Another difficulty arises since the model should include combined temperature and salinity effects. It is not immediately obvious how a realistic equation of state for sea water can be incorporated into an isopycnal model. In wind-driven isopycnal models, such as that of Bleck and Boudra (1986), it is implicitly assumed that the equation of state relates only temperature to density and that salinity is not a dynamically active tracer or else is assumed to be constant. The consequence is that isotherms coincide with isopycnals. However, here it is not sufficient to include equations for velocity and layer thickness, which is the vertical distance between two specified isopycnic surfaces. Additional equations for heat and salt content are required. Without vertical mixing and salinity as an active tracer, temperature and consequently potential density are constant in time, since they are a priori constant within the same layer. The prediction equation for temperature reduces to $(\partial T)/(\partial t) = 0$ since all gradients along isopycnals vanish. In consequence, neither a prognostic nor a diagnostic equation is necessary to control potential density, temperature, or salinity. The basic difference in the model described here is its aim of using a realistic equation of state, which is nonlinear in temperature, salinity, and pressure. This gives rise to the following conceptual problem. Consider an advection of temperature whose gradient is balanced by an appropriate salinity gradient to obtain a spatially constant potential density along the model interfaces. In practice, discretization errors in the advection formulation yield an alongisopycnal artificial mixing of temperature and salinity. Due to the nonlinearity of the equation of state this results in a drift of the potential density and thus a drift of the coordinates. This is called cabbeling. For clarification, besides the artificial cabbeling due to advecting discretization errors a physical cabbeling also exists that is simply the result of alongisopycnal mixing.

In order to maintain the chosen coordinate system, it is necessary to compensate for the coordinate drift by suitable redefinition of the coordinates. Because temperature and salinity vary along isopycnals, equations for temperature and salinity are necessary to control heat and salt conservation. On the other hand, it must be postulated that the potential density coordinates must be maintained.

There are two possible ways to resolve this problem. The first is to reconfigure the coordinates after each time step and determine the resulting mass exchange rates necessary to maintain the coordinates. However, this introduces a mixing process that possibly exceeds physical realism. The other possibility, which is adopted here, is to connect the process of maintaining the isopycnic coordinates with the parameterization of cross-isopycnal mixing. It is formulated by entraining water into each layer out of the adjacent upper and lower layers. The ratio of these two entrainment rates is treated as a free parameter, while the sum of the two entrainment rates is derived from the available turbulent kinetic mixing energy. Given the condition that the instantaneous potential density must be kept at the prescribed potential density, an appropriate choice of the ratio of both entrainment rates is able to compensate for the potential density drift caused by an alongisopycnal discretization error of the advection terms and the alongisopycnal diffusion. The instantaneous potential density is thereby the result of the predicted potential temperature and salinity. The entrainment into a given layer appears as a detrainment for the adjacent upper and lower layers and thus does not alter the potential density in the adjacent layers (for details see section 2d). The underlying idea is to introduce some bookkeeping within each layer for the potential density errors. The simplest way to achieve that is to write the equations as if potential density is allowed to vary arbitrarily. This ensures that dynamically other-

wise ignored errors in the potential density do not lead to a violation of conservation properties as conversion between mean potential and kinetic energy. The isopycnal coordinates are then introduced through the back door by appropriate formulations of all vertical exchange processes, such as vertical mixing and convection.

More theoretically, the source of this problem is the employment of an underdetermined set of equations. To describe the ocean state, the flow and pressure field has to be determined. The pressure is a function of temperature and salinity. In addition, however, the location of interfaces is predicted. Thus, the pressure field is not uniquely defined by one set of model variables but by an infinite number of them. As an example, consider a vertical profile of potential density. One can find an infinite number of layer-mean potential densities with appropriate layer thicknesses to represent the same profile in discretized space. The underdetermined nature of the equations appears, for instance, as freedom of how to mix vertically. Vertical mixing can be achieved by moving the coordinates, altering the carried quantities, or by any compromise of it. This freedom is then used to select that representation of the vertical profile which yields a constant potential density within the same layer.

Further complications arise through disappearing and reappearing layers below the mixed layer or at the variable bottom of the ocean. An algorithm is needed to treat the time dependence of the spatial extent of each layer (for details see section 2f).

The concept of the model used here can be summarized as follows. The ocean model is divided up into two regions: the upper and the lower ocean. The former is represented by a mixed layer. The lower ocean is discretized by isopycnic surfaces where cross-isopycnic mixing and convection are explicitly included in the lower ocean. The atmospheric fluxes are distributed within a fully active mixed layer and are modified by a fully coupled sea ice model with rheology.

a. Ocean model

Ignoring, for the moment, dissipative processes the basic quantities that should be conserved are momentum, energy, mass, potential vorticity, heat and salt content, and possible tracer concentrations. Momentum, mass, and heat and salt content are easily conserved if the flux form of the equations is chosen. Bleck (1974, 1978, 1979) investigated the conservation of energy and potential vorticity in a generalized coordinate system. Isentropic coordinates for the atmosphere or isopycnic coordinates for the ocean are only special cases of these coordinates. Since Bleck's results concerning the atmospheric lee cyclogenesis behind mountains or the Gulf Stream dynamics in the ocean are so noteworthy, this scheme will be used for momentum transport here. Following Bleck and Boudra (1981), potential vorticity can be conserved after some manipulations of the advection and Coriolis terms. Total energy cannot be conserved exactly here, as it is the intention to use the flux form of the equations of motion. This is not crucial, as the model ocean will be much more diffusive than the real ocean due to the additional diffusion required for computational stability reasons. Thus, energy will be dissipated anyway. Therefore, it is defendable to relax the total energy conservation condition with the advantage of now being able to conserve momentum, mass, heat, salt, and potential vorticity. Following Arakawa (1966, 1972), the equations are discretized in the horizontal using the B-grid.

The basic equations are formulated in flux form as conservative equations for the vertical mean of the mass flux $\boldsymbol{\Psi}_k = \rho v h_k$, the mass content $\Phi_k = (\rho h)_k$, the heat content $\Theta_k = (\theta \rho h)_k$, and the salt content $\Pi_k = (S\rho h)_k$ in a column of the *kth* layer:

$$\frac{\partial}{\partial t}\boldsymbol{\Psi}_k = -\nabla(\mathbf{v}_k\boldsymbol{\Psi}_k) - h_k\nabla p_k - \mathbf{f}\times\boldsymbol{\Psi}_k + \nabla\cdot A_k^m\nabla\boldsymbol{\Psi}_k + (\mathbf{w}\rho\mathbf{v})_k^{k+} + (\mathbf{w}\rho\mathbf{v})_k^{k-} - (\mathbf{w}\rho\mathbf{v})_{k+}^{k} - (\mathbf{w}\rho\mathbf{v})_{k-}^{k} + \boldsymbol{\tau}_k^{k-} + \boldsymbol{\tau}_k^{k+} \quad (1)$$

$$\frac{\partial}{\partial t}\Phi_k = -\nabla\cdot\boldsymbol{\Psi}_k + (w\rho)_k^{k+} + (w\rho)_k^{k-} - (w\rho)_{k+}^{k} - (w\rho)_{k-}^{k} + R_k^{P-E} \quad (2)$$

$$\frac{\partial}{\partial t}(\Theta)_k = -\nabla\cdot(\Theta\mathbf{v})_k + \nabla\cdot A_k^s\nabla(\Theta)_k + \frac{Q_k}{c_p} + (w\rho\theta)_k^{k-} + (w\rho\theta)_k^{k+} - (w\rho\theta)_{k-}^{k} - (w\rho\theta)_{k+}^{k} \quad (3)$$

$$\frac{\partial}{\partial t}(\Pi)_k = -\nabla\cdot(\Pi\mathbf{v})_k + \nabla\cdot A_k^s\nabla(\Pi)_k + R_k^{\mathrm{ICE}} + (w\rho S)_k^{k-} + (w\rho S)_k^{k+} - (w\rho S)_{k-}^{k} - (w\rho S)_{k+}^{k}. \quad (4)$$

The terms $(\mathbf{w}\rho\mathbf{v})$, $(w\rho)$, $(w\rho\theta)$, and $(w\rho S)$ describe exchange processes of mass fluxes, mass itself, and heat and salt content between neighboring layers. The different kinds of exchange processes are entrainment/detrainment, vertical exchange as cross-isopycnal mixing and convection. The terminology $(\ldots)_k^l$ indicates a transfer from the *lth* layer into the *kth* layer, where $l = k-$ represents the next upper and $l = k+$ the next lower (physically present) layer; N is the number of layers, the index k starting with $k = 1$ in the uppermost layer (mixed layer). Note that the terms that appear as entrainment out of the adjacent layers into layer k and as detrainment out of layer k into the adjacent layers finally help to keep the potential densities close to the prescribed one (see section 2d). All terms in which $1-$ or $N+$ occur are set to zero, except for the term $\boldsymbol{\tau}_1^{1-}$, which represents the surface wind stress, and the term $\boldsymbol{\tau}_N^{N+}$, which represents the bottom stress.

The Coriolis parameter f in Eq. (1) is related to the earth's rotation

$$f = 2\Omega \sin(\varphi) \quad \text{with} \quad \Omega = \frac{2\pi}{86\,164}, \tag{5}$$

where Ω is the angular velocity of the rotating earth. The equations are formulated on the sphere. All metric terms that are the result of the transformation onto the curvilinear spherical grid are, for example, listed in Semtner (1986). Note that all operators taken as two-dimensional as derivatives in the vertical vanish through the use of Lagrangian coordinates.

The stress $\boldsymbol{\tau} = (\tau_x, \tau_y)$ between neighboring layers is parameterized as

$$\boldsymbol{\tau}_k^l = c_d \rho_a \sqrt{\Delta \mathbf{v}^2}\, \Delta \mathbf{v} \quad \text{with}$$
$$\Delta \mathbf{v} = (\Delta u, \Delta v) = (u_l - u_k, v_l - v_k); \tag{6}$$

ρ_a is the surface air density. Since observed surface stresses are used, the surface drag coefficient does not need to be specified. For the internal stresses, $c_d = 10^{-4}$ and at the bottom $c_d = 10^{-3}$.

In order to complete the equations, in situ values of the density ρ, temperature T, salinity S, and pressure P are related by the equation of state for sea water (UNESCO 1981), written symbolically as

$$\rho_k = \rho_k(T_k, S_k, P_k). \tag{7}$$

After discretization, the in situ pressure in the first layer is given as a vertical mean by

$$P_1 = \frac{g}{2} \Phi_1, \tag{8}$$

where $g = 9.8$ m s^{-2} is the gravitational constant. In all deeper layers the in situ pressure P_k is given by

$$P_k = P_{k-1} + \frac{g}{2}(\Phi_{k-1} + \Phi_k). \tag{9}$$

One of the conceptual problems in layer models is how to determine the horizontal pressure gradient. An obvious choice would be to take neutral surfaces as coordinates. However, technical limitations of computing and storing large amounts of density data for computing pressure gradients, without any reduction error, onto a reference level makes it advisable to postpone a more accurate solution to a later state of the model. Meanwhile, potential density is used. Note that in situ densities cannot be taken, as each grid point within the same layer is located at a different depth. In the case of constant potential density within each layer, horizontal pressure gradients can be derived from the slope of the interfaces alone (see Bleck and Boudra 1981). In this model, however, potential densities are allowed to be variable within all layers so that additional terms appear, which reflect the generation of a pressure gradient in the presence of a horizontal gradient of potential density. Remember that the deviation from a reference potential density will be small; this will be guaranteed by the vertical mixing processes. The diagnostic equation for the pressure gradient is

$$\nabla p_k = g\sigma_{\theta 1}\Big(\sum_{l=k}^{N} \nabla h_l + \nabla D\Big) + g \sum_{l=1}^{k-1} \nabla(h\sigma_\theta)_l + g \frac{h_k}{2} \nabla \sigma_{\theta k} - g(\sigma_{\theta k} - \sigma_{\theta 1}) \sum_{l=1}^{k-1} \nabla h_l, \tag{10}$$

where D is the height of the topography above some reference level. Due to the nonlinearity of the equation of state, the pressure gradients are weakly dependent on the choice of the reference level, which for simplicity is chosen here to be the surface.

The in situ temperature T_k is calculated by inverting the formula of Bryden (1973), which relates potential temperature to temperature, salinity, and pressure:

$$\theta_k = \theta_k(T_k, S_k, P_k). \tag{11}$$

By combining the UNESCO formula for density with the formula for potential temperature, the potential density σ_θ is defined by using the potential temperature and salinity in the same layer and reducing it to a specified reference pressure level.

The forcing terms Q_k and R_k in Eqs. (2) and (3) represent the heat flux and the freshwater flux, respectively. Thereby, R_k^{P-E} ($R_k^{P-E} = 0$ for $k > 1$) is the freshwater flux due to precipitation minus evaporation, and R_k^{ICE} due to the sea ice–ocean coupling. $c_p = 4180$ J (kg K)$^{-1}$ is the specific heat capacity of water. The freshwater flux does not appear in the salinity equation since it is written in flux form.

The total heat flux into the mixed layer is given by

$$Q_1 = Q_H + Q_L + Q_l + Q_s[1 - \gamma \exp(-h_1/h_B)] \tag{12}$$

and consists of the sensible heat flux Q_H, the latent heat flux Q_L, the net heat flux by longwave radiation Q_l, and the heat flux Q_s due to insolation. Following Paulson and Simpson (1977), $h_B = 23$ m is the decay length scale for the absorption of solar radiation, and $\gamma = 0.42$ defines the fraction of the insolation that is not immediately absorbed at the surface but penetrates into the ocean. These values reflect clear water type I. This means that when all upper layers are shallow enough, deeper layers gain heat due to insolation. The heating rates of all deeper layers are defined by

$$Q_k = Q_s[\exp(-\sum_{l=1}^{k-1} h_l/h_B) - \exp(-\sum_{l=1}^{k} h_l/h_B)]\gamma. \tag{13}$$

The coefficients A_k^m and A_k^s represent the spatial and time-dependent diffusion for momentum, heat, and salt. Following Bleck's tradition, the horizontal diffusion coefficient for temperature and salinity is parameterized according to Smagorinsky (1963) by relating it to the deformation of the flow field:

$$A^s = c\left[\left(\frac{\partial u}{\partial x} - \frac{\partial v}{\partial y}\right)^2 + \left(\frac{\partial u}{\partial y} + \frac{\partial v}{\partial x}\right)^2\right]^{1/2} + A_0^s. \quad (14)$$

Here, c is set to 5×10^9 m^2 to obtain realistic diffusion coefficients, typically of order 10^4 m^2 s^{-1} with a minimum diffusion coefficient of $A_0^s = 10^3$ m^2 s^{-1}. The diffusion coefficient for momentum depends on the grid spacing, which is variable in longitude and latitude. It is made smaller in areas of a high resolution in order not to destroy narrow structures there. The formulas for the x and y components of the momentum diffusion coefficient $A^m = (A_x^m, A_y^m)$ are

$$A_x^m = \frac{\Delta x^2}{T_0 \cos\varphi} + A^s \quad (15)$$

$$A_y^m = \frac{\Delta y^2}{T_0 \cos\varphi} + A^s. \quad (16)$$

Here Δx is the zonal grid distance at a latitude φ, and Δy the meridional grid distance. The $\cos\varphi$ terms ensure that the damping time for $2\Delta x$ and $2\Delta y$ waves have the same scale, independent of whether waves at the equator or near the North Pole are considered. Here T_0 is set to 4×10^6 s, which results in a momentum diffusion coefficient in the range of 10^4 m^2 s^{-1} at the equator. It becomes smaller toward the pole, thereby taking account of the converging coordinates and the higher resolution, which requires less diffusion for numerical stability. That diffusion is chosen to be stronger for momentum than for the scalar quantities is governed primarily by the need to couple the two separate solutions in the B-grid (this problem does not appear in the equations for Θ and S).

b. *Mixed-layer model*

A mixed layer (ML) is the result of turbulence produced by wind stirring and surface buoyancy fluxes. Temperature, salinity, velocities, and tracers are then uniformly distributed in the vertical. Such a surface boundary layer is included here. Since quantities in a layer model are assumed to be constant vertically in each layer, only the mixed-layer depth (MLD) appears as unknown. On the other hand, the MLD is not influenced only by local mixing but also by horizontal convergence of mass or heat. Therefore, the full dynamics represented by Eqs. (1) to (4) are considered and completed by a parameterization for the vertical mass transfer and that of related quantities across the ML base. The uppermost layer is used as the layer with a thickness that is always nonzero and an arbitrary instantaneous potential density σ_θ (see Fig. 1). In all deeper layers it is intended to keep the instantaneous potential density σ_θ at a prescribed value, henceforth called σ_θ^*. This quantity is constant within each layer and depends only on the layer index.

1) PHYSICAL BACKGROUND

Following Kraus and Turner (1967), the assumption leading to a mixed-layer model is that wind-induced breaking waves and buoyancy fluxes produce turbulent kinetic energy (TKE), which is partly converted into mean potential energy (MPE) and partly dissipated. One of the main problems is that the different kinds of mixed-layer models are tuned towards particular local conditions [e.g., Ocean Station Papa; see Martin (1985)]. A general formulation that is able to treat quite different mixed-layer regimes in different parts of the ocean is not available at present. The essential difficulty is to simulate the deep mixed layer in the western parts of the tropical oceans and to explain with the same set of parameters the normally shallower mixed layer in midlatitudes, where much stronger wind stirring and convection through surface cooling occurs. A summary of some of the difficulties concerning earlier ML models is given in Gaspar (1988).

Here, results of sensitivity studies with different ML-model formulations are briefly discussed in order to justify the ML-model version developed here. Results for the Atlantic Ocean domain and one for the already existing global ocean indicate that the Niiler (1975) model generates a too shallow mixed layer of about 20 m in the western parts of the equatorial oceans. In higher latitudes the ML is too deep, as numerical experiments also indicate for the western part of the North Atlantic. The error patterns coincide roughly with the TKE production due to wind stirring [see u_*-fields of Bunker (1976); Oberhuber (1988)]. Strongest TKE production appears south and east of Newfoundland during winter and spring. It appears that TKE due to wind stirring is dissipated with depth.

Niiler and Kraus (1977) formulated a model that includes an additive term for the dissipation of TKE. This modification allowed them to simulate a cyclostationary state. But this model also fails to overcome the shortcoming of a mixed layer that is too shallow in lower latitudes. For reasons that are not yet understood, less TKE is needed for mixing at higher latitudes than at lower ones. Garwood (1977) tried to resolve this problem by including a Coriolis parameter–dependent damping term. The problem with both of these ad hoc parameterizations is that, even without buoyancy fluxes, the ML is limited to some depth. The basic form of their entrainment relation is

$$wg'h = c_1 u_*^3 + c_2 hB - c_3 h, \quad (17)$$

where c_1, c_2, and c_3 are arbitrary tuning coefficients; u_* is the friction velocity; and B is the buoyancy flux. By setting $w = 0$ this results in the Monin–Obukhov length h_M:

$$h_M = \frac{c_1 u_*^3}{c_3 - c_2 B}. \quad (18)$$

For a sufficiently strong damping parameter c_3, which

is required to keep the mixed layer realistically shallow in many areas, h_M always yields a positive solution for the MLD. Independent of the internal stability, the MLD cannot exceed h_M. As already noted by Deardorff (1983), this type of parameterization allows the occurence of unstable stratification (due to cooling) that is not removed by convection (deepening of the ML). The newer theory of Garwood et al. (1985a,b) proposed an $\Omega_y \tau_x$ term, which acts as a source of TKE in easterly winds and as a sink in westerly winds. Consequently, this model generates a deep mixed layer in western parts of the equatorial oceans, but it enhances mixing in the trade wind area, so that the MLD in the latter area is overestimated.

From these preliminary experiments it is obvious that another form is required to describe the latitudinal dependence of dissipation of TKE. Proceeding from the equator poleward, it must decay more rapidly than the cosine function of the Ω_y term. On the other hand, it should not suppress convection. The hypothesis was, therefore, introduced that TKE decays exponentially with depth with a length scale h_s given by the Ekman scale. Thus, the TKE production term is multiplied with an exponential function so that the entrainment relation takes the form:

$$wg'h = \exp\left(-\frac{h}{h_s}\right) \times (\text{TKE surface production}). \tag{19}$$

If the stability g' approaches zero, the entrainment rate increases independently of how small the exponential function becomes. If the right-hand function is expanded around a mean MLD h_o, one obtains:

$$wg'h = \left(1 - \frac{h - h_0}{h_s}\right) \exp\left(-\frac{h_0}{h_s}\right) \times (\text{TKE surface production}). \tag{20}$$

This is a similar structure [compare with Eq. (17)] to that used in the models of Niiler and Kraus (1977), Garwood (1977), and Gaspar (1988). Thus, their models can be understood as Taylor expansions of the subsequently presented ML model with an appropriate definition of h_s, c_1, c_2, and c_3. Since the annual mixed-layer variation at Ocean Station Papa is small due to the strong thermocline in the North Pacific, a Taylor expansion is justified in this region, but it is obvious that at high latitudes in the North Atlantic or in the Circumpolar Current, it will fail if the decay function is nonlinear.

2) MIXED-LAYER EQUATIONS

The mixed-layer model finally selected for this study was the result of numerous sensitivity experiments, in which the best simulation of the seasonal cycle for various mixed-layer models was optimized by tuning the model parameters using an inverse method. The models of Niiler (1975), Niiler and Kraus (1977), Garwood (1977), and Garwood et al. (1985a,b) were tested in this manner. The present model gave a reduced rms error for the seasonal cycle of the ML between 25°S and 65°N for the Atlantic. The equation for the entrainment rate w is

$$\begin{aligned} wg'h - w\,\mathrm{Ri}_{\mathrm{crit}}(\Delta u^2 + \Delta v^2) &= 2m_o a u_*^3 + \Gamma b h B_I + (1-\Gamma) h b (B - \gamma B_s) \\ &\quad + (1-\Gamma)\gamma b B_s [h(1 + \exp(-h/h_B)) \\ &\quad - 2h_B(1 - \exp(-h/h_B))], \end{aligned} \tag{21}$$

where

$$g' = g\frac{\sigma_{\theta 1+} - \sigma_{\theta 1}}{\sigma_{\theta 1}}(1-\Gamma) + \Gamma g'_I \tag{22}$$

$$B = \frac{g}{c_p \rho^2}(\alpha Q + \beta R) \tag{23}$$

$$R = \frac{c_p \rho}{S}(P - E) \tag{24}$$

$$B_s = \frac{\alpha g}{c_p \rho^2} Q_s; \tag{25}$$

g' is the reduced gravity between the mixed layer and the next layer below; $\mathrm{Ri}_{\mathrm{crit}}$ is the critical Richardson number (set to 0.25); B is the total buoyancy flux through the surface; Q the total heat flux; R the corresponding equivalent heat flux due to the freshwater flux; $P - E$ denotes precipitation minus evaporation; B_s the buoyancy flux due to the solar radiative heat flux Q_s; and α, β are the analytically determined expansion coefficients with respect to temperature and salinity.

The entrainment/detrainment rate w is related to the transfer rates w_k^l in the equations (1) to (4) by

$$w = \begin{cases} w_1^{+1}, & \text{if} \quad w > 0 \\ w_{+1}^1, & \text{if} \quad w < 0. \end{cases} \tag{26}$$

The sea ice model described subsequently has some influence on the relation for entrainment. In the presence of sea ice, $\Gamma = 1$, otherwise $\Gamma = 0$. B_I is taken as buoyancy flux and g'_I as reduced gravity, if sea ice is present. Both parameters are defined in section 2e.

The first term on the left-hand side of Eq. (21) describes the production of mean potential energy (MPE), and the second is the production term of mean kinetic energy (MKE) by entrainment. On the right-hand side, the first term represents the TKE production due to wind stirring (u_* denotes the friction velocity), the following describe the influence of the surface-buoyancy fluxes for the ice-covered and ice-free conditions, respectively. The last term, which is only nonzero for ice free cases, represents the influence of pen-

etrating solar radiation on the total buoyancy flux (Denman and Miyake 1973). The free parameter m_o is set to 1.2. This value is approximately the same as that derived from laboratory experiments. In the relation for the entrainment rate the weighting coefficients a, b are defined as exponential decay functions:

$$a = \exp[-hf/(\kappa u_*)] \tag{27}$$

$$b = \begin{cases} \exp[-hf/(\kappa u_*)], & \text{if } B < 0 \\ \exp[-hf/(\mu u_*)], & \text{if } B > 0, \end{cases} \tag{28}$$

where $\kappa = 0.4$ and $\mu = 2$.

Two different length scales are chosen, a larger scale for those terms which create deepening and a smaller one for those which reduce the MLD. This follows from the heuristic argument that wind stirring generates only $\overline{u'w'}$ terms at the surface, whereas $\overline{w'T'}$ terms are also produced as a result of positive buoyancy fluxes. In this case, they act as a source of TKE due to the generation of unstable stratification. This kind of turbulence penetrates into the ocean and creates on its part again $\overline{u'w'}$ turbulence. Thus, positive buoyancy fluxes are assumed to be more efficient than wind-induced turbulence.

One of the preliminary findings during the optimization efforts was to find $\kappa = 0.39$, which surprisingly corresponds to the von Kármán constant if the thickness of a turbulent boundary layer is estimated by $\kappa u_*/f$. The constant μ, which also was found by optimization, is significantly larger. Note that μ is the only coefficient that is not known approximately and therefore can be used for tuning.

An important property of the dissipation formulation presented here is that at the equator TKE generated at the surface penetrates down to the mixed-layer base without being partly dissipated. If $f = 0$, then $a = 1$. The mixed layer in the western parts of the equatorial oceans will be sufficiently thick as long as m_o is large enough. The value chosen for m_o is much larger than used by Niiler (1975), but in this model this is compensated for by letting TKE decay towards higher latitudes, thus giving a comparable TKE at the mixed-layer base at Ocean Station Papa. Proceeding from the equator poleward, the Ekman length decreases rapidly. Therefore, the strong trade winds will not lead to an unrealistically thick mixed layer. This was one of the deficiencies in experiments with the model proposed by Garwood et al. (1985a,b). In midlatitudes the strong westerlies will not give large mixed-layer thicknesses, since the decay length scale is about 30 m there.

In the retreat phase of the mixed layer the depth is determined by setting $w = 0$ in Eq. (21) and solving for h. The resulting equation for the Monin–Obukhov length h_M in the case of no sea ice yields:

$$2m_o u_*^3 + h_M(B - \gamma B_s) + \gamma B_s\{h_M[1 + \exp(-h_M/h_B)] - 2h_B[1 - \exp(-h_M/h_B)]\} = 0. \tag{29}$$

The solution for h_M is determined iteratively with a Newton method. A second diagnostic calculation is carried out as soon as the flow becomes unstable due to excessive vertical shear. In this case, a minimum depth h_{Ri} is defined through:

$$h_{Ri} = \mathrm{Ri}_{crit}(\Delta u^2 + \Delta v^2)/g'. \tag{30}$$

As a result, there are two constraints that limit the MLD. First, the MLD cannot be deeper than the Monin–Obukhov length, and second, it cannot be shallower than h_{Ri}. If the two constraints contradict each other, h_{Ri} is taken as criterion. This means that as long as the MLD is smaller than h_M and larger than h_{Ri}, the MLD is not altered by these diagnostic calculations, but as soon as the MLD becomes smaller than h_{Ri} or larger than h_M, the corresponding diagnostic quantity is taken.

3) Coupling of the mixed-layer and the isopycnal model

Figure 2 demonstrates how layers disappear and reappear during the seasonal cycle. Starting with a rather shallow mixed layer (Fig. 2a), water is entrained during the deepening phase (beginning with autumn) from the second layer into the mixed layer. As the mixed layer deepens (Fig. 2b), the second layer loses mass until it has drained dry (Fig. 2c). Now water is entrained from the next deeper layer (Fig. 2d). If the atmospheric conditions allow the entrainment regime to change to a detrainment regime (beginning with spring), a new shallow mixed layer is formed, which

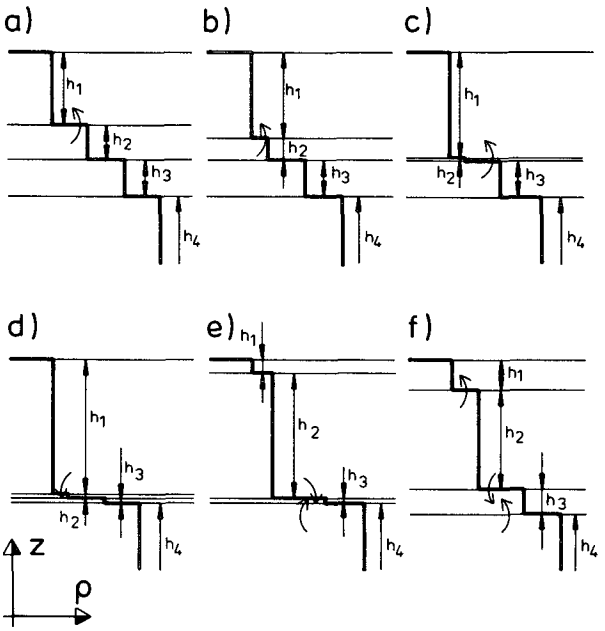

FIG. 2. Seasonal cycle of layer thicknesses at and below the mixed layer. For details see text.

is determined diagnostically (Fig. 2e). The detrained water masses of the old mixed layer are assigned to other layers. During this phase, a vanished layer may reappear formally through vertical mixing (Fig. 2e) or by detrainment into that layer.

The conceptual problem now is to select one of the layers below the ML into which the detrained water mass may be pumped. The solution would be unique if the potential density of the detrained water coincides with the prescribed potential density σ_θ^* of the underlying physically existing layer UL. In this case, the detrained water would not alter the potential density in that layer and therefore would not destroy the model's coordinate system. But, in general, this situation will not occur since the ML potential density is allowed to develop arbitrarily.

The following strategy was developed through the need to maintain the isopycnal coordinates, that is, to keep σ_θ at or as close as possible to the prescribed σ_θ^*. In the first step, it is asked whether the currently calculated σ_θ is larger or smaller than the prescribed σ_θ^*. The difference expresses the currently existing error in the isopycnal coordinates. Then use is made of the fact that detrainment occurs only if negative buoyancy fluxes as result of a positive heat and freshwater flux yield a steadily decreasing potential density in the ML. This means that a steady decrease of σ_θ in the ML will also lead to a steady decrease of σ_θ in the UL when water of the ML is continuously mixed down into the same UL. The following decision has been found to work satisfactorily. In the case of $\sigma_\theta > \sigma_\theta^*$, the detrained water is injected into UL. Thus, the lighter detrained water is mixed with the UL water, which was originally too heavy when compared with its prescribed potential density. As a result, water in the UL becomes lighter and therefore steadily approaches its σ_θ^*. In the other case, $\sigma_\theta < \sigma_\theta^*$, or if initially UL already contains the correct σ_θ, the detrained water is pumped into the next upper, not yet physically existing, layer with $h = 0$. Since this layer corresponds naturally to a smaller σ_θ^* compared with the σ_θ of the ML, the detrained water will now be too heavy for this layer. However, because of the steady decrease of σ_θ of the detrained water, the instantaneous σ_θ in the flooded zero layer will decrease towards its σ_θ^*. After having reached the corresponding σ_θ^*, the detrained water is injected into the next upper, not yet physically existing, layer. In this manner, an arbitrary number of layers may be flooded until detrainment stops owing to changed atmospheric conditions. At the end of the detrainment regime several flooded layers remain. Because of the finite time steps, σ_θ^* is never reached exactly. But as long as the time step is small compared with the time scale of the atmospheric forcing, the remaining errors in the flooded layers will be negligible. Only the layer that was the last one into which water was detrained might contain a significant deviation from σ_θ^*. But this layer is the first one entrained into the ML and is, so far, only physically active during a short period.

c. *Parameterization of surface fluxes*

The surface fluxes required by the model are the fluxes of momentum, heat, fresh water, turbulent kinetic energy, and buoyancy. Required datasets are surface air temperature, sea surface temperature, relative humidity, cloudiness, the time-averaged absolute wind speed and its standard deviation, wind stress, rainfall, and surface salinity. Esbensen and Kushnir (1981) calculated global surface heat fluxes on a coarse 5° × 5° grid. Based on the higher-resolution COADS [Comprehensive Ocean–Atmosphere Data Set; Woodruff et al. (1987)], Wright (1988) prepared data on a 2° × 2° grid, which is sufficient for forcing an OGCM. These fields represent a 30-year climatology from 1950 to 1979. Using this data source Oberhuber (1988) developed and tuned parameterizations of all fluxes required for forcing an ocean model, such as heat, buoyancy, fresh water, and turbulent kinetic energy. The computed heat fluxes are in surprising agreement with Isemer and Hasse (1987), who optimized their scheme for the North Atlantic only.

1) Parameterization of surface heat fluxes

The total surface heat flux Q consists of the contribution due to shortwave radiation Q_s, longwave radiation Q_l, sensible heat flux Q_H, and latent heat flux Q_L. The turbulent surface heat fluxes, namely the sensible and latent heat fluxes, are estimated by the bulk formulae

$$Q_H = \rho_a c_{p,\text{air}} c_H V (T_a - T_s) \tag{31}$$

$$Q_L = \rho_a L_w c_L V (q_a - q_s), \tag{32}$$

where T_a is the air temperature, T_s the sea surface temperature, q_a the air specific humidity, and q_s the specific humidity close to the surface, which is assumed to be the saturated value; $c_{p,\text{air}} = 1005$ J kg^{-1} K^{-1} is the specific heat of air, and $L_w = 2.5 \times 10^6$ J kg^{-1} the latent heat of evaporation. The specific humidity q is given by the water vapor pressure e and the atmospheric surface pressure p. In the following relations, (33)–(39), the unit for e and p is pascal and the unit for T is kelvin:

$$e = 611 \times 10^{7.5(T-273.16)/(T-35.86)} \tag{33}$$

$$q = \frac{0.622\, e}{p - 0.378 e}. \tag{34}$$

From this $q_s = q(p, e(T_s))$ and $q_a = q(p, r \times e(T_a))$ are obtained, where r is the relative humidity. The bulk coefficients, c_H and c_L, are calculated as proposed by Large and Pond (1982). The respective formulae are given in the next section.

The net longwave radiation at the surface is taken from Berliand and Berliand (1952):

$$Q_l = 4\epsilon\sigma T_a^3 (T_a - T_s) - \epsilon\sigma T_a^4 (0.39 - 0.05\sqrt{e/100})(1 - \chi n^2), \tag{35}$$

where $\epsilon = 0.97$ is the emissivity of water, $\sigma = 5.67 \times 10^{-8}$ W m^{-2} K^{-4} the Stefan–Boltzmann constant, and n the relative cloud cover. In order to account for different properties of different cloud types, χ varies linearly with latitude, as proposed by Budyko (1974).

The insolation is calculated from the daily averaged heat flux at the top of the atmosphere and is then corrected after Zillmann (1972) for relative humidity and inclination. Parkinson and Washington (1979) used Zillmann's formula for modeling the sea ice, while Hsiung (1985, 1986) used the empirical formula of Seckel and Beaudry (1973). However, since the latter formula is valid in a latitudinal band only, Zillmann's formula, which can be used in global models, was selected here. Following Reed (1977), the insolation is reduced by a cloudiness factor. In contrast to Esbensen and Kushnir (1981), the cloudiness correction of Berliand (1960) is not used, since this underestimates insolation at high cloud cover, as pointed out by Weare et al. (1981). The resulting relations required to compute the daily mean downward shortwave radiative flux Q_s are

$$\cos\eta = \sin\delta \sin\varphi + \cos\delta \cos\varphi \cos t \quad (36)$$

$$\sin\eta_{\text{noon}} = \sin\delta \sin\varphi + \cos\delta \cos\varphi \quad (37)$$

$$\kappa = 1 - 0.62n + 0.0019\eta_{\text{noon}} \quad (38)$$

$$Q_s = \alpha \frac{\kappa\gamma}{2\pi} \int_{t_1}^{t_2} \frac{S_0 \cos^2\eta}{r(\cos\eta + 2.7)e(T_a)/p + 1.085\cos\eta + 0.1} \left(\frac{\bar{d}}{d}\right)^2 dt. \quad (39)$$

Here, $S_0 = 1370$ W m^{-2} is the solar constant, and η the solar elevation. The constant γ is chosen as 0.94 corresponding to an albedo of 0.06; $\alpha = 0.9$ is a tuning coefficient, d denotes the distance between the sun and earth, and $\bar{d}$ its annual average. Following Paltridge and Platt (1976), the ratio $(\bar{d}/d)^2$ is estimated in terms of the Julian day β:

$$\left(\frac{\bar{d}}{d}\right)^2 = 1.00011 + 0.00128\sin(\beta) + 0.034221\cos(\beta) + 0.000077\sin(2\beta) + 0.000719\cos(2\beta). \quad (40)$$

The declination δ (in radians), needed to compute η, is given by

$$\delta = 0.006918 + 0.070257\sin(\beta) - 0.399912\cos(\beta) + 0.000907\sin(2\beta) - 0.006758\cos(2\beta) + 0.00148\sin(3\beta) - 0.002697\cos(3\beta). \quad (41)$$

Variations in the distance between sun and earth account for slightly more than 3% of the variations in the net global solar radiation.

2) TRANSFER COEFFICIENTS

The bulk coefficients are taken from Large and Pond (1981, 1982). Although the method is discussed in detail in both papers, all relations are listed again to clarify which equations are used here:

$$c_H = \frac{c_{HN}\sqrt{c_M/c_{MN}}}{1 - c_{HN}\kappa^{-1}c_{MN}^{-1/2}\psi_H(Z/L)} \quad (42)$$

$$c_L = \frac{c_{LN}\sqrt{c_M/c_{MN}}}{1 - c_{LN}\kappa^{-1}c_{MN}^{-1/2}\psi_L(Z/L)} \quad (43)$$

$$\sqrt{c_M/c_{MN}} = (1 - \sqrt{c_{MN}}\kappa^{-1}\psi_M(Z/L))^{-1} \quad (44)$$

$$c_{MN} = \frac{\kappa^2}{\ln^2(Z/Z_0)} \quad (45)$$

$$c_{HN} = 0.0327\frac{\kappa}{\ln(Z/Z_0)} \quad (46)$$

$$c_{LN} = 0.0346\frac{\kappa}{\ln(Z/Z_0)} \quad (47)$$

$$Z_0 = c_{\text{Char}}\frac{u_*^2}{g} \quad (48)$$

$$u_*^2 = c_M u^2 \quad (49)$$

$$T_0 = T(1 + 1.7 \times 10^{-6}Tq). \quad (50)$$

Here c_M, c_H, and c_L are the transfer coefficients for momentum, sensible, and latent heat, respectively. The subscript N denotes the transfer coefficient for neutral conditions. For stable conditions it is

$$\psi_M = \psi_H = \psi_L = -7(Z/L) \quad (51)$$

$$(Z/L) = -\frac{70Z}{u^2T_0}(\Delta\theta + 2.5 \times 10^{-6}T_0^2\Delta q), \quad (52)$$

while for unstable conditions it is

$$\psi_M = 2\ln[(1 + X)/2] + \ln[(1 + X^2)/2] - 2\arctan X + \pi/2 \quad (53)$$

$$\psi_H = \psi_L = 2\ln[(1 + X^2)/2] \quad (54)$$

$$X = (1 - 16(Z/L))^{1/4} \quad (55)$$

$$(Z/L) = -\frac{100Z}{u^2T_0}(\Delta\theta + 1.7 \times 10^{-6}T_0^2\Delta q), \quad (56)$$

where Δq is the difference between the specific humidity of air, and the sea surface and $\Delta\theta$ is the potential temperature difference.

The only difference from Large and Pond's work is that c_{MN} is not fitted against data using ad hoc chosen curves but by tuning the Charnock constant. The Eqs. (45), (48), and (49) describe the dependence of the neutral drag coefficient c_{MN} on the friction velocity u_*, the von Kármán constant $\kappa = 0.4$, the height of the measurement Z, and Charnock's constant c_{Char}. In order to obtain a drag coefficient of about 1.15×10^{-3} for neutral conditions at 10 m s^{-1}, c_{Char} should be set to 0.0064. The resulting dependence of the neutral drag coefficient c_{MN} on the wind speed u is similar to Large

and Pond's result and within the accuracy of the measurements presented by Large and Pond. However, as outlined by Oberhuber (1988), c_{Char}, in fact, was set to 0.032 to compensate for the underestimation of the transfer coefficient resulting from the application of monthly mean values instead of instantaneous values.

3) Relation to Newtonian cooling

Despite the complexity of the formulae for the heat flux, the relations between SST and the resulting heat flux are essentially of Newtonian type (see also Haney 1971), however, with a strong spatially variable coupling coefficient $\partial Q/\partial T$. If the heat flux Q is linearized with respect to the observed sea surface temperature, one obtains

$$Q(T) = Q(\text{SST}) - \frac{\partial Q(\text{SST})}{\partial T}(\text{SST} - T), \quad (57)$$

where T may be considered as the modeled surface temperature and $Q(T)$ as the resulting surface heat flux. After introducing an equivalent temperature T^* defined by

$$T^* = \text{SST} - Q(\text{SST})\left(\frac{\partial Q(\text{SST})}{\partial T}\right)^{-1}, \quad (58)$$

Eq. (57) can be rewritten as

$$Q(T) = -\frac{\partial Q(\text{SST})}{\partial T}(T^* - T). \quad (59)$$

The temperature difference $(T^* - T) = -Q(\text{SST})/(\partial Q(\text{SST})/\partial T)$ depends on the observed heat flux and can therefore exceed 3 K for typical situations in equatorial upwelling areas (Q = 100 W m^{-2}, $(\partial Q)/(\partial T)$ = 30 W m^{-2} K^{-1}) or even 10 K in Gulf Stream and Kuroshio areas (Q = 600 W m^{-2}, $(\partial Q)/(\partial T)$ = 60 W m^{-2} K^{-1}). Initial tests using SST instead of the equivalent temperature T^* did indeed exhibit systematic errors. Therefore, it appears advisable to derive fluxes from parameterizations that employ observed atmospheric data rather than SST data and take account of the strong spatial dependence of $\partial Q/\partial T$. A further advantage of using atmosphere rather than surface data is that the SST data already contain the time lag due to the oceanic inertia of about 2 months. If a model is forced with such data, the time lag would be introduced twice.

4) Evaluation of the net freshwater flux

Because rainfall is not sufficiently well known, a Newtonian formulation was applied to the observed sea surface salinity:

$$R_1^{P-E} = \rho_1 \delta \frac{S_{\text{obs}} - S_1}{S_1}, \quad (60)$$

where $\delta = 5 \times 10^{-6}$ m s^{-1} is the time constant with which the actual salinity relaxes towards the observed salinity S_{obs}. This approach circumvents the drift, which could occur through the lack of any stabilizing feedback if the ocean is forced with slightly incorrect observed rainfall and evaporation.

In the presence of sea ice, changes of the salinity in the mixed layer are not permitted by this parameterization. In order to maintain the observed salinity (at least in terms of the annual mean), the mean salinity is determined from the mixed-layer thickness and the sea ice. By employing this artificial salinity instead of the observed one the required net freshwater flux is calculated, which is added to the ice as snowfall. This ensures that the mixed-layer salinity returns to the observed value when all the ice has melted.

5) Estimate of turbulent kinetic energy input

Monthly mean absolute wind $\bar{V}$ and its standard deviation $\sigma(V)$ were prepared from COADS by Wright (1988). The standard deviation is required for accurately evaluating the time-averaged third power of the friction velocity u_*, occurring in the relation for the entrainment rate. Since $\bar{u}_*^3$, determined from the monthly mean absolute wind $\bar{u}$ only, is much smaller than the required $\overline{u_*^3}$, the effective u_*^3 must be determined by the additional use of the monthly mean standard deviation of the absolute wind. By assuming that the amplitude of the fluctuations is not too large compared with the mean wind, the effective u_*^3 can be approximated by:

$$u_*^3 = \left(\frac{c_d \rho_a}{\rho}\right)^{3/2} \bar{V}(\bar{V}^2 + 3\sigma^2(V)). \quad (61)$$

The standard deviation of the wind is generally of the order of half the mean wind strength, so that the expression yields roughly twice as much kinetic energy as would result from the mean wind alone.

d. Parameterizations of internal diffusion

Vertical diffusion is needed to prevent fronts from becoming too strong and to allow a steady flow across isopycnals as a precondition for deep meridional overturning. Thus, a parameterization for vertical diffusion in the interior ocean is introduced by allowing mass to be transferred between neighboring layers. An explicit convection mixing procedure is also included.

1) Vertical mixing/coordinate maintainance

In order to formulate vertical mixing, some kind of mass transfer rate w has to be specified. This could be defined at each layer interface by transferring mass between two neighboring layers. However, as an additional constraint the potential density has to be maintained in each isopycnic layer.

To satisfy this constraint, the mass exchange of a given layer with both the upper and lower layer is con-

sidered simultaneously. As indicated in Fig. 3, the basic picture is that each layer obtains mass from its neighboring layers by an entrainment process and, at the same time, loses mass to these layers by a detrainment process. Each of the transferred water masses $\Delta t\rho w$ in a time step Δt carries information relating to momentum, temperature, salinity, or other tracer concentrations. For illustration of the problem, it is assumed in Fig. 3 that the upward and downward mass transfer across an interface are identical. However, since a coordinate displacement is allowed in the present model concept, the relations $(\rho w)_k^{k+} = -(\rho w)_{k+}^k$ and $(\rho w)_k^{k-} = -(\rho w)_{k-}^k$ have to be relaxed. The notation for $(\rho w)_k^{k+}$, $(\rho w)_k^{k-}$, $(\rho w)_{k-}^k$, and $(\rho w)_{k+}^k$ is the same as that used for the continuity equation (2). Figure 4 shows how the vertical mixing is generalized. The sum of the four mass transfer rates yields the net change of the mass content of the layer with index k. The entrainment and detrainment processes are treated in the same way as in the mixed-layer model. If water is transferred from one layer into a neighboring layer, the velocity, temperature, and salinity are changed only in the layer into which a water mass is transferred (entrainment) but not in the layer from which the water mass is removed. The final result appears as decomposition of the net transfer rate from one layer into an adjacent one. For each layer two entrainment and two detrainment rates have to be determined. Only the entrainment rates are of importance for the tendency equation for temperature and salinity. Since the detrainment rates are identical to the entrainment rates of the adjacent layers, it is sufficient to determine the entrainment rates only. Thus, two unknown quantities appear for each layer, which reflects the underdetermined nature of Eqs. (1)–(4).

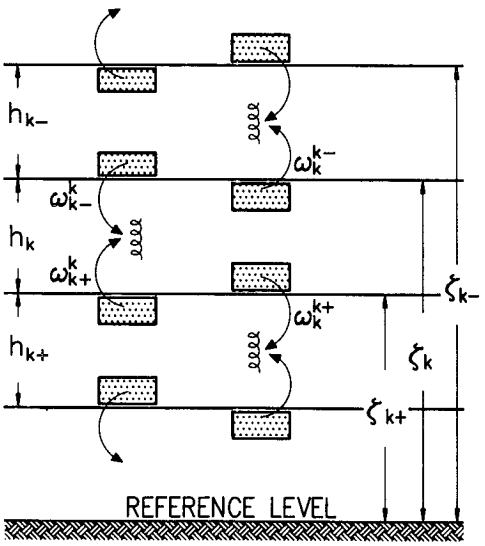

FIG. 3. Design of the parameterization of vertical diffusion. In z-coordinate models the relation $w_k^{k+} = w_{k+}^k$ and $w_k^{k-} = w_{k-}^k$ ensures that coordinates ζ (= interfaces in layer models) remain unchanged.

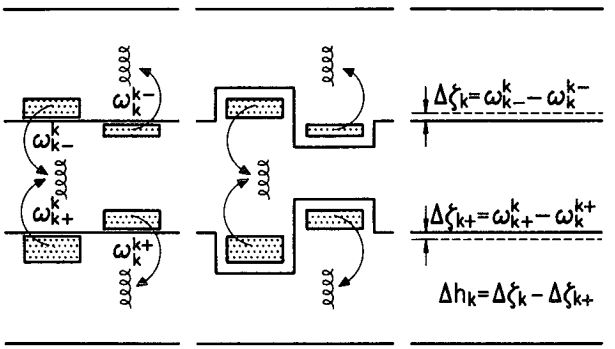

FIG. 4. Modification of the parameterization of vertical diffusion. Compared to Fig. 3 the exchanged water masses are now not of equal amount. The result is a net change of the interfaces.

Following the mixed-layer parameterization, it is assumed that turbulent kinetic energy is converted into mean potential energy via a u_*^3 term. However, for the interior ocean the friction velocity u_* is not adequately known. The contribution to u_* from fluctuations (eddies, transient internal waves) can be much greater than from the mean-flow contribution. Therefore, a constant $u_* = 0.5$ cm s^{-1} in the entire ocean is chosen. The value was tuned to obtain the best thermocline.

If water is entrained only from above or only from below, the resulting equations for the entrainment rates w_k^{k-*} and w_k^{k+*} are

$$w_k^{k-*} = \frac{2m_0 u_*^3}{g'_{k-} h_k} \tag{62}$$

$$w_k^{k+*} = \frac{2m_0 u_*^3}{g'_{k+} h_k}. \tag{63}$$

The problem is underdetermined, since one is free to choose how much is to be entrained from above or from below. If a free parameter α for this unknown ratio is introduced the equation for the total entrainment rate w_k is given by

$$w_k = (1 - \alpha) w_k^{k-*} + \alpha w_k^{k+*} \tag{64}$$

with individual entrainment rates

$$w_k^{k-} = (1 - \alpha) w_k^{k-*} \tag{65}$$

$$w_k^{k+} = \alpha w_k^{k+*}. \tag{66}$$

After substituting these entrainment rates into the momentum, mass, heat, and salt equations, the free parameter α can now be chosen to maintain the potential density of the layer at the prescribed value σ_θ^*, at the same time compensating the potential density drift due to artificial and physical cabbeling. In order to balance these errors, α must be made space and time dependent. The equation that determines α reads

$$[h_k + \Delta t(w_k^{k-} + w_k^{k+})]\sigma_{\theta k}^* = h_k \sigma_{\theta k} + \Delta t w_k^{k-} \sigma_{\theta k-} + \Delta w_k^{k+} \sigma_{\theta k+}, \tag{67}$$

stating that the potential density at the new time level should be equal to the prescribed value $\sigma^*_{\theta k}$. This equation was derived under the assumption that the potential density of a mixed water mass is the layer thickness weighted average of the potential densities of the unmixed water masses. Together with the Eqs. (65) and (66) this yields as the final equation for α:

$$\alpha = \frac{h_k(\sigma^*_{\theta k} - \sigma_{\theta k}) + \Delta t w_k^{k-*}(\sigma^*_{\theta k} - \sigma_{\theta k-})}{\Delta t w_k^{k-*}(\sigma^*_{\theta k} - \sigma_{\theta k-}) - \Delta t w_k^{k+*}(\sigma^*_{\theta k} - \sigma_{\theta k+})}. \tag{68}$$

2) CONVECTION

At first sight it appears that it is not necessary to include a procedure for explicit convection in this model. Both the mixed-layer and interior ocean mixing formulation should prevent the development of unstable stratification.

However, if the stability between ML and UL tends towards zero, the entrainment rate increases drastically. The time step extrapolation together with small values of the exponential function for the dissipation of TKE can then lead to situations where the stratification has already become unstable, but the underlying layer has not yet vanished. In this case, the unstable stratification is removed by vertical mixing. All quantities are set to their vertical average over the ML and the UL.

The consequence of this procedure is that the potential density in the UL increases with respect to its σ^*_θ. For the purpose of setting bounds for this potential density error $(\sigma_\theta - \sigma^*_\theta)$, the following procedure was found to work satisfactorily: if σ_θ in the UL approaches σ^*_θ of the next deeper layer, the UL is totally entrained into it. Ignoring nonlinear temperature and salinity effects in the equation of state, the instantaneous potential density σ_θ in this next deeper layer is unchanged. Since the former UL has now lost its entire mass, the original third layer from the top becomes the new UL. If instability persists for this layer, the same process is repeated for the next pair of layers, the ML and the new UL. After convection has finished, new zero layers remain between the ML and the UL, which now has bigger vertical extent.

In the isopycnal part of the model, layers are initially stably stratified. The stability is maintained as long as the entrainment/detrainment mechanism for maintaining the initial potential density in each layer works correctly. Unstable stratification due to vertical mixing occurs only under extreme cases of vertical temperature and salinity gradients when the assumption of a linear equation of state conflicts with the nonlinear equation of state, which in fact, is used. If in rare cases unstable stratification arises through either situation, velocities, temperatures, and salinity are set equal to their mean values over the two adjacent unstable stratified layers. Layer thicknesses are not altered.

e. Sea ice model

Ice is an important boundary condition for the high-latitude ocean. The seasonal cycle of ice thickness and ice extension influences the heat budget at the ocean surface and the internal stratification. During cold periods, freezing ice ejects salt into the mixed layer and thereby contributes to the production of heavy deep water. During warm periods, melting ice decreases the salinity in the mixed layer and therefore contributes to a stabilization of the upper ocean.

1) EQUATIONS

Parkinson and Washington (1979) developed a model for the sea ice using the free drift approximation. Hibler (1979) showed that a realistic rheology yields improved results. This type of model demonstrates its reliability in runs for the Arctic and the Antarctic. The results of Hibler and Bryan (1987), who coupled such a sea ice model with rheology to the GFDL model, also gave some motivation to include a similar model. For a number of technical reasons, such as the use of spherical coordinates and the momentum and mass-conserving flux form of the equations that permits an easier treatment of the ice edge, it was decided to develop a new model based on the same physics as in Hibler's model.

The basic equations for the ice flux $\mathbf{v}h$, for the ice mass h, and the ice concentration q are

$$\frac{\partial}{\partial t}\mathbf{v}h = \nabla \cdot A\nabla \mathbf{v}h - \mathbf{f} \times \mathbf{v}h - gh\nabla\Gamma + \frac{\boldsymbol{\tau}_a}{\rho_I} + \frac{\boldsymbol{\tau}_0}{\rho_I} + h\mathbf{F}_v \tag{69}$$

$$\frac{\partial}{\partial t}h = \nabla \cdot A\nabla h - \nabla \cdot \mathbf{v}h + F_h \tag{70}$$

$$\frac{\partial}{\partial t}q = \nabla \cdot A\nabla q - \nabla \cdot \mathbf{v}q + F_q, \tag{71}$$

where $\boldsymbol{\tau}_a$ and $\boldsymbol{\tau}_0$ are the surface wind stress and the stress at the bottom of the ice, respectively, and Γ is the sea surface. In these equations the transport of momentum has been neglected. Here A is a constant diffusion coefficient currently set to be 2000 $m^2\ s^{-1}$; $\mathbf{f}$ is the Coriolis parameter; $\mathbf{F}_v$, F_h, and F_q are the forcing functions for the momentum, mass, and ice concentration; $\mathbf{F}_v$ represents the sea ice rheology, defined to be viscous plastic; F_h the ice thickness change; and F_q the change of the ice concentration due to external heat fluxes. Following Hibler's notation, the forcing functions are defined by

$$F_{vx} = \frac{\partial}{\partial x}\left[(\eta + \zeta)\frac{\partial u}{\partial x} + (\zeta - \eta)\frac{\partial v}{\partial y} - \frac{P}{2}\right] + \frac{\partial}{\partial y}\left[\eta\left(\frac{\partial u}{\partial y} + \frac{\partial v}{\partial x}\right)\right] \tag{72}$$

$$F_{vy} = \frac{\partial}{\partial y}\left[(\eta + \zeta)\frac{\partial v}{\partial y} + (\zeta - \eta)\frac{\partial u}{\partial x} - \frac{P}{2}\right] + \frac{\partial}{\partial x}\left[\eta\left(\frac{\partial u}{\partial y} + \frac{\partial v}{\partial x}\right)\right] \quad (73)$$

$$\Delta = \left[\left(\frac{\partial u}{\partial x}\right)^2 + \left(\frac{\partial v}{\partial y}\right)^2\right]\frac{1 + e^2}{e^2} + \left(\frac{\partial u}{\partial y} + \frac{\partial v}{\partial x}\right)^2 \frac{1}{e^2} + 2\frac{\partial u}{\partial x}\frac{\partial v}{\partial y}\frac{e^2 - 1}{e^2} \quad (74)$$

$$P = \frac{P^* h}{\rho_I} \exp[-C(1 - q)] \quad (75)$$

$$\zeta = \frac{P}{\max(2\sqrt{\Delta}, \epsilon_0)} \quad (76)$$

$$\eta = \frac{\zeta}{e^2}. \quad (77)$$

Parts of the operators on the right-hand side can be identified as diffusion operator, with two diffusion coefficients, the bulk viscosity ζ, and the shear viscosity η, which are highly dependent on the flow field. However, additional terms occur that cross-couple the velocity components. Similar to Hibler (1979), the free parameters have been chosen as $P^* = 10^4$ N m^{-2}, $e = 2$, $C = 20$, and $\epsilon_0 = 2 \times 10^{-7}$; $\rho_I = 900$ kg m^{-3} is the constant ice density.

2) THERMODYNAMIC FORCING

The net heat flux through the ice into the ocean is parameterized by

$$Q_I = \alpha q \frac{T_s - T_1}{h}. \quad (78)$$

Here, T_s is the skin temperature of the ice surface and h/q the current thickness of each ice floe. It is assumed that no snow layer exists and that the ice is homogeneous. The conductivity parameter α is chosen to be 2 W (mK)$^{-1}$.

The heat flux through the ice surface is calculated by the equilibrium condition that there is no heat flux divergence. This yields the ice surface temperature T_s by an implicit definition:

$$Q_A(T_s, \cdots) - Q_I\left(T_s, T_1, \frac{h}{q}\right) = 0, \quad (79)$$

where Q_A is the atmospheric heat flux defined in section 2c(1) and Q_I the heat flux through an ice floe. From this equation, the surface temperature T_s is calculated by iteration. The resulting change in the local ice thickness due to thermodynamics is then given by the sum of the heat flux Q from the atmosphere into the ice-free ocean, the heat flux Q_I through the ice, and the flux induced by the entrainment rate w:

$$F_h = -\frac{qQ_I + (1 - q)Q_1}{\rho c_{pm}} - \frac{|w| + w}{2}\frac{c_p}{c_{pm}}(T_{1+} - T_1), \quad (80)$$

where $c_{pm} = 334$ kJ kg^{-1} is the latent heat of fusion.

The forcing function of the ice concentration equation differs slightly from Hibler's formulation and is evaluated by

$$F_q = \begin{cases} F_h(1 - q)/h_0, & \text{if } F_h > 0 \\ F_h q/2h, & \text{if } F_h < 0. \end{cases} \quad (81)$$

The free parameter h_0 is set to 0.5 m. The goal of this ad hoc parameterization is to relate the change of the ice concentration with that of the ice thickness during melting ($F_h < 0$), while during freezing ($F_h > 0$) the concentration change is related with an area that is not covered by thick ice but contains thin ice of thickness h_0. Dependent on the ice concentration, the ocean obtains its forcing either through leads from the atmosphere or through the sea ice.

3) EXTENSIONS IN THE MIXED-LAYER MODEL

In the presence of sea ice the buoyancy flux B_I from the atmosphere into the mixed layer is determined by

$$B_I = (qQ_I + (1 - q)Q_1)\frac{g(S_1 - S_I)}{c_{pm}\rho\sigma_\theta}\left.\frac{\partial\sigma_\theta}{\partial S}\right|_{\theta,\rho}, \quad (82)$$

where S_I is the ice salinity, set to be 0.5%. This expression implies that the heat flux through the ice is associated with a freshwater flux, because ice keeps the mixed-layer temperature at the freezing point. Furthermore, with $B_s = 0$, it is assumed that no solar radiation penetrates through the ice. Finally, following Lemke (1987), the reduced gravity in the entrainment equation (21) is modified by

$$g'_I = g\left[\frac{\sigma_{\theta 1+} - \sigma_{\theta 1}}{\sigma_{\theta 1}} + \left(\left.\frac{\partial\sigma_\theta}{\partial\theta}\right|_{S,p} + \frac{c_p(S_1 - S_I)}{c_{pm}\sigma_\theta}\left.\frac{\partial\sigma_\theta}{\partial S}\right|_{\theta,p}\right)(\theta_{1+} - \theta_1)\right]. \quad (83)$$

Compared to the entrainment equation without sea ice there are additional mechanisms. Entrainment provides some heat flux into the mixed layer. This flux is exactly balanced by a heat flux due to melting or freezing ice in order to keep the mixed-layer temperature at the freezing point. Finally, this freshwater flux induces a buoyancy flux.

4) SEA ICE–OCEAN SALT COUPLING

During freezing, salt is ejected out of the ice but is not confined to the ML alone. It is assumed that a fraction of this ejected salt penetrates more deeply with

a length scale that depends on the stratification in the surface layers. A higher stability should thereby give a shorter length scale. The following ad hoc parameterization for a salt transfer out of the mixed layer into all deeper layers ($k = 2, \cdots, N$) is chosen as

$$R_k^{\mathrm{ICE}} = \frac{|F_h| + F_h}{2}\rho_1(S_1 - S_I)\left[\exp\left(-\frac{\sigma_{\theta k} - \sigma_{\theta 1}}{h_p}\sum_{l=1}^{k-1} h_l\right) - \exp\left(-\frac{\sigma_{\theta k+} - \sigma_{\theta 1}}{h_p}\sum_{l=1}^{k} h_l\right)\right], \quad (84)$$

where $h_p = 20$ kg m^{-2} is a free parameter tuned to obtain a reasonable model response. The salinity budget in the ML is the result of the salinity gain due to freezing ice and the salinity loss due to the downward transfer of a fraction of the salinity gain. The salinity change in the ML is given by

$$R_1^{\mathrm{ICE}} = \rho_1(S_1 - S_I)\left[F_h - \frac{|F_h| + F_h}{2} \times \exp\left(-\frac{\sigma_{\theta 1+} - \sigma_{\theta 1}}{h_p} h_1\right)\right]. \quad (85)$$

Thus, water formed from melting ice ($F_h < 0$) is completely mixed within the ML since $R_k^{\mathrm{ICE}} = 0$ for $k = 2, \cdots, N$, but freezing ice injects a fraction of the salt into deeper layers. This allows the model to build up a salinity stratification in the Arctic basin, although in the annual mean there is a net transport of salt from the sea ice through the ML into the deeper ocean. The balance between this downward transport, vertical diffusion, and other transports yields an equilibrium state of the salinity stratification in areas covered by sea ice.

f. Numerical schemes

The numerics of the present model are more complex than in a standard ocean model. Besides the usual space and time discretization problems, a number of additional problems arise. First, the basic equations are strongly nonlinear to the variation of layer thicknesses. Second, vanishing layers must be treated by means of an algorithm that does not affect conservation properties. Third, a sea ice model must be coupled to the mixed layer and the mixed layer to the isopycnal model. Finally, all techniques must be vectorizable with the option to parallelize, too.

1) Discretization in space

The most discussed problem of isopycnal models is the matter of the treatment of coordinates that intersect the bottom or the surface. The interfaces in the isopycnic part of the model physically disappear either into the mixed layer (where the isopycnals run in the vertical) or into the topography, for example, at the continental shelf or at sea mounts. Formally, a layer that has physically disappeared is retained in the model as a layer with zero thickness. Grid points in this layer do not contain mass, but still hold dummy values for temperature, salinity, and other quantities. The key to realizing this concept is to succeed in decoupling a zero layer from the ocean by an appropriate boundary condition. Furthermore, physical processes that change the location where an isopycnal disappears/reappears or that create water masses with a not yet existing potential density must have their counterpart in a technique that allows the shifting of boundaries or the flooding of zero layers. Such a method must work under the constraint that the ocean dynamics does not feed back to the dummy values that are kept in the zero layer.

Following Arakawa (1966) a *B*-grid with no-slip boundary condition is taken, as shown in Fig. 5. Since fluxes are diffused instead of velocities, a linearly decreasing layer thickness together with a linearly decreasing flux yields a constant velocity even at the last velocity grid point before the boundary (see Fig. 7).

A method is required that allows the displacement of boundaries under the conservation of mass, heat, salt, and momentum. The major reason why the well-established FCT algorithm is not used relates to the fact that the layerwise correction of a layer thickness has no regard to resulting changes of the sea surface elevation and to the baroclinic structure of the vertical modes. Therefore, the following method was developed.

The idea of variable boundaries has been outlined in Oberhuber (1986) and is shown in Fig. 6. The hatched areas mark layers with zero thickness. Note that the position of the boundaries corresponds to the cross section in Fig. 1. The technique is illustrated in Fig. 7. Consider a velocity point that is the last one

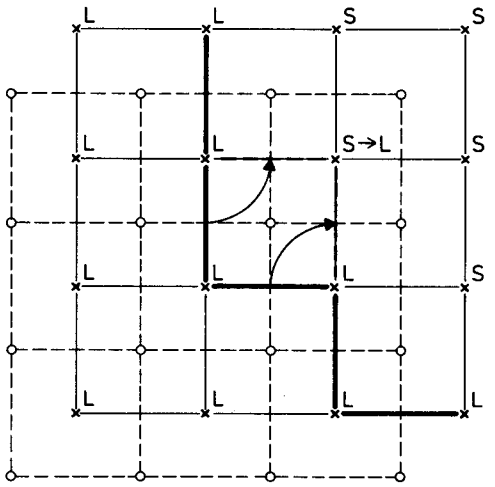

FIG. 5. Schematic horizontal layout of the *B* grid: "*L*" stands for land points, "*S*" for sea points. Circles denote mass points, crosses velocity points. The thick solid line denotes the boundary at a certain time level. The dashed line marks the updated boundary at the new time level in the case of outflow out of the enclosed mass cell.

before the layer disappears at the topography. Because of the grid staggering the next mass point lies on the topography. The evaluation of the pressure gradient at that velocity point contains a dependence on the topography slope since the baroclinic part of the pressure gradient depends on the slope of all upper interfaces. This would yield a spatial discretization producing enormous artificial accelerations since the topography can change drastically within any chosen resolution. This problem is resolved by interpreting the distribution of layer thicknesses as steps, as shown in Fig. 7b.

There are three types of velocity grid points. A velocity point is surrounded by cells that either all contain mass ($h > 0$), are all massless ($h = 0$), or at least one contains mass and at least another one is massless. In the first case such a velocity point is part of the ocean, whereas in the second case it is part of a zero layer and has no connection to ocean points. However, in the third case, a decision cannot be made a priori. This preliminary freedom is used to define criteria that ensure a physically correct treatment of moving boundaries. The physical mechanisms that control the boundary definition are horizontal mass convergence and vertical cross-interfacial mass flux determined by detrainment and vertical mixing. The proposal is to prevent the development of a negative mass content, and this is achieved as follows: If a massless point ($h = 0$) is surrounded by at least one mass-containing point ($h > 0$), as in Figs. 7a,b, then the considered massless point may receive mass from this neighboring mass-containing point if the intermediate velocity point results in a convergence at the massless point. In this case, the intermediate velocity is defined as a sea point. In the case when mass loss is diagnosed in the massless cell, the intermediate velocity point is defined as a land point, so that this cell is closed off from the ocean and therefore does not receive a negative mass content.

The remaining problem is to predict the velocities at those points that are required to define the boundary conditions in order to connect massless cells only with the ocean if finally an inflow will be predicted. For this purpose the following method was developed. Since only the sign of the mass convergence is important, the momentum and continuity equations are integrated explicitly forward. From this preliminary result, the location of the boundaries is derived and finally taken to carry out one time step. This causes no additional overhead, since in the semi-implicit time integration scheme the required terms have to be computed anyway. This procedure is repeated at the beginning of each time step. Thus, the distribution of land and sea points is updated every time step. An arbitrary number of grid cells may be switched off and on. However, in the case when horizontal (along isopycnal) convergence tends to flood several massless cells, the procedure allows for the connection of only one cell per time step.

For the two-dimensional case, Fig. 5 shows a simple example of how a mass cell is switched off. On the basis of the updating process for the old boundaries (solid thick line), the new boundaries (broken thick line) are determined. In summary, a finite mass cell remains part of the ocean as long as it contains mass and is switched off from the ocean only if it has already lost its entire mass and is still losing mass (thus avoiding a negative mass content). Massless cells become part of the ocean if convergence is predicted and remain massless if the flow is divergent.

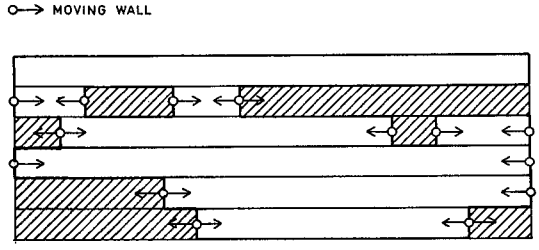

FIG. 6. Schematic cross section of the model layout. Shaded areas denote zero layers. Arrows indicate moving boundaries. The wall positions correspond to Fig. 1.

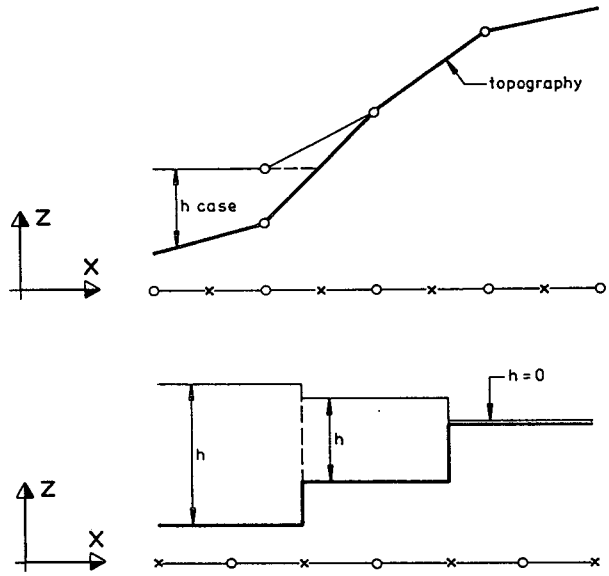

FIG. 7. Vertical cross section at a velocity point with a physically disappearing layer. Circles denote mass points, crosses velocity points. Upper panel (a) shows that the spatial distribution of interface height is interpreted as a linear function. Lower panel (b) shows that the spatial distribution of interface height is interpreted as steps.

2) DISCRETIZATION IN TIME

In order to obtain large time steps a predictor–corrector technique is adopted. Each of these steps is based on a semi-implicit method. For details see Kwizak and Robert (1971). The method yields an unconditionally stable time integration scheme with respect to all external and internal waves, advection, diffusion, and mixed-layer physics. In the predictor step, the pressure

gradient, Coriolis term, and the vorticity part of the momentum advection [see 2f(4)] in the momentum equation, the flux divergence in the continuity equation, and the advection and diffusion terms in the equation for potential temperature and salinity are treated implicitly.

In order to demonstrate how this technique is adjusted here, the derivation of the wave equation is explained in detail. The predictor–corrector scheme is outlined more generally in section a of the Appendix. In the first step, the momentum equation is discretized in time by using a centered Euler scheme (note that this works more efficiently with the commonly used leapfrog scheme). The x and y components of the momentum equation (1) then read:

$$(\rho uh)^{n+1} = (\rho uh)^n - \frac{\Delta t}{2} h^{n+1} \frac{\partial}{\partial x} p^{n+1} + \frac{\Delta t}{2} (f+\zeta)(\rho vh)^{n+1} + F^n_{\rho uh} \quad (86)$$

$$(\rho vh)^{n+1} = (\rho vh)^n - \frac{\Delta t}{2} h^{n+1} \frac{\partial}{\partial y} p^{n+1} - \frac{\Delta t}{2} (f+\zeta)(\rho uh)^{n+1} + F^n_{\rho vh}, \quad (87)$$

where $F^n_{\rho uh}$ and $F^n_{\rho vh}$ represent all the remaining terms taken at time level n. In the next step both equations are written for $(\rho uh)^{n+1}$ or $(\rho vh)^{n+1}$ only by cross referencing the flux components. This yields

$$(\rho uh)^{n+1} = F^{*n}_{\rho uh} - \left[\frac{\Delta t}{2} h^{n+1} \frac{\partial}{\partial x} p^{n+1} + \frac{\Delta t^2}{4} (f+\zeta) h^{n+1} \frac{\partial}{\partial y} p^{n+1}\right] \Big/ \left[1 + \frac{\Delta t^2}{4} (f+\zeta)^2\right] \quad (88)$$

$$(\rho vh)^{n+1} = F^{*n}_{\rho vh} - \left[\frac{\Delta t}{2} h^{n+1} \frac{\partial}{\partial y} p^{n+1} - \frac{\Delta t^2}{4} (f+\zeta) h^{n+1} \frac{\partial}{\partial x} p^{n+1}\right] \Big/ \left[1 + \frac{\Delta t^2}{4} (f+\zeta)^2\right], \quad (89)$$

where $F^{*n}_{\rho uh}$ and $F^{*n}_{\rho vh}$ are the abbreviations of

$$F^{*n}_{\rho uh} = (\rho uh)^n + \left\{F^n_{\rho uh} + \frac{\Delta t}{2} (f+\zeta)\left[(\rho vh)^n + F^n_{\rho vh}\right]\right\} \Big/ \left[1 + \frac{\Delta t^2}{4} (f+\zeta)^2\right] \quad (90)$$

$$F^{*n}_{\rho vh} = (\rho vh)^n + \left\{F^n_{\rho vh} - \frac{\Delta t}{2} (f+\zeta)\left[(\rho uh)^n + F^n_{\rho uh}\right]\right\} \Big/ \left[1 + \frac{\Delta t^2}{4} (f+\zeta)^2\right]. \quad (91)$$

If the continuity equation is discretized in the same manner as the momentum equation this yields

$$(\rho h)^{n+1} = (\rho h)^n - \frac{\Delta t}{2}\left[\frac{\partial}{\partial x}(\rho uh)^{n+1} + \frac{\partial}{\partial y}(\rho vh)^{n+1}\right] + F^n_{\rho h}, \quad (92)$$

where $F^n_{\rho h}$ represents all the remaining terms taken at time level n. If the flux divergence is now eliminated by using (88) and (89), an equation for the layer thickness h only can be obtained:

$$(h^{n+1}_k - h^n_k)\frac{\rho^n_k + \rho^{n+1}_k}{2} = F^{*n}_{\rho h} - (\rho^{n+1}_k - \rho^n_k)\frac{h^n_k + h^{n+1}_k}{2} + \frac{\Delta t^2}{4}\frac{\partial}{\partial x}\frac{h^{n+1}_k}{1 + \Delta t^2 (f+\zeta)^2/4}\frac{\partial}{\partial x} p^{n+1}_k + \frac{\Delta t^2}{4}\frac{\partial}{\partial y}\frac{h^{n+1}_k}{1 + \Delta t^2 (f+\zeta)^2/4}\frac{\partial}{\partial y} p^{n+1}_k + \frac{\Delta t^2}{4}\frac{\partial}{\partial x}\frac{h^{n+1}_k \Delta t (f+\zeta)/2}{1 + \Delta t^2 (f+\zeta)^2/4}\frac{\partial}{\partial y} p^{n+1}_k - \frac{\Delta t^2}{4}\frac{\partial}{\partial y}\frac{h^{n+1}_k \Delta t (f+\zeta)/2}{1 + \Delta t^2 (f+\zeta)^2/4}\frac{\partial}{\partial x} p^{n+1}_k. \quad (93)$$

An identity (see section b of the Appendix) therefore is used to separate ρ and h from the product ρh. The quantity $F^{*n}_{\rho h}$ denotes the explicit part of the wave equation (93), defined by

$$F^{*n}_{\rho h} = F^n_{\rho h} - \frac{\Delta t}{2}\left(\frac{\partial}{\partial x} F^{*n}_{\rho uh} + \frac{\partial}{\partial y} F^{*n}_{\rho vh}\right). \quad (94)$$

Together with the equation of state (6) and the relation for the in situ pressure (7) and (8), Eq. (93) determines h^{n+1}_k. The density at the new time level is updated during the iteration by using the layer thickness and the previously determined potential temperature and salinity. Finally, after having found the solution for layer thickness and density, the mass fluxes are obtained from (88) through (91).

The wave equation is formulated as a system of linear equations in x and z and iterated in y, which is an application of the "line iteration" method. The wave equation consists of quadratic terms, which represent the inertia–gravity waves, and mixed derivatives, which

correspond to Rossby waves. Because of the large time steps used in this model [$\Delta t(f+\zeta)/2 > 1$], the mixed derivative terms dominate the quadratic terms, so that simple iteration methods used for Laplacian-type equations cannot be used. Based on the fact that an iteration converges if the mean diagonal elements dominate over the neighboring diagonals, a method has been developed that calculates for every grid point an optimal relaxation coefficient by changing the mean diagonal element artificially without changing the final solution.

3) Discretization of advection for T and S

For this study, an advection scheme similar to that employed by Smolarkiewicz (1982) is used, namely an implicit version of the scheme presented by Crowley (1968). The scheme is less diffusive than the upstream scheme and avoids the tendency of centered difference schemes to overshoot. It can be understood as a simple quasi-Lagrangian scheme in which higher-order terms are neglected in the Taylor expansion of the problem.

If f is an arbitrary quantity, the scheme is given by:

$$f^{n+1} = f^n - \Delta t\left(u^n \frac{\partial}{\partial x} f^* + v^n \frac{\partial}{\partial y} f^*\right) + \Delta t \frac{\partial}{\partial x}\left[u^n \frac{\Delta t}{2}\left(u^n \frac{\partial}{\partial x} f^* + v^n \frac{\partial}{\partial y} f^*\right)\right] + \Delta t \frac{\partial}{\partial y}\left[v^n \frac{\Delta t}{2}\left(u^n \frac{\partial}{\partial x} f^* + v^n \frac{\partial}{\partial y} f^*\right)\right] + F \quad (95)$$

$$f^* = \frac{f^n + f^{n+1}}{2}, \quad (96)$$

where F is some forcing function representing residual terms in one of the temperature or salinity equations. The scheme is second order in space and time.

4) Treatment of the momentum transport and Coriolis term

Bleck and Boudra (1981) tested a potential vorticity and energy-conserving advection scheme for momentum. Their idea is adjusted here to the requirements of the implicit technique used to achieve large time steps. The momentum advection and Coriolis terms on the right-hand side of the momentum equation (1) are rewritten in the following way for the x component:

$$-\frac{\partial}{\partial x}(uu\rho h) - \frac{\partial}{\partial y}(vu\rho h) + fv\rho h + v\rho h \frac{u\tan\phi}{r} = -\frac{\rho h}{2}\left(\frac{\partial u^2}{\partial x} + \frac{\partial v^2}{\partial x}\right) - u\left(\frac{\partial u\rho h}{\partial x} + \frac{\partial v\rho h}{\partial y}\right) + v\rho h \frac{u\tan\phi}{r} + (f+\zeta)v\rho h \quad (97)$$

and for the y component

$$-\frac{\partial}{\partial x}(uv\rho h) - \frac{\partial}{\partial y}(vv\rho h) - fu\rho h - u\rho h \frac{u\tan\phi}{r} = -\frac{\rho h}{2}\left(\frac{\partial u^2}{\partial y} + \frac{\partial v^2}{\partial y}\right) - v\left(\frac{\partial u\rho h}{\partial x} + \frac{\partial v\rho h}{\partial y}\right) - u\rho h \frac{u\tan\phi}{r} - (f+\zeta)u\rho h, \quad (98)$$

where ζ is the relative vorticity. The terms on the right-hand sides represent, in this order, energy gradients, momentum convergence, curvature, and an altered Coriolis term, which now contains the absolute vorticity instead of the Coriolis parameter only. This term is included in the implicit formulation of the wave equation (93), which is the predictor step. The residual terms are treated implicitly in the first corrector step, which also contains the momentum diffusion terms. Since the momentum components are cross coupled in the equations, the linear equation in x is formulated simultaneously for both velocity components. See also section c of the Appendix for a discussion of the physical implications.

5) Numerical formulation of the sea ice model

The sea ice model works on the same spherical grid and with the same time step as the ocean model. The predictor–corrector method in connection with the semi-implicit technique is applied. First, diffusion of

ice thickness and ice concentration are determined implicitly. In this step the flux divergence of ice thickness and ice concentration are still taken explicitly forward. In the next step, the stress and Coriolis terms are treated implicitly. In the final correction step the sea ice rheology in the flux equation is treated implicitly. The coupling of the predictor and two corrector steps follows the same procedure as outlined in section 2f(2). All iterations are carried out in the y direction only, since a system of linear equations is solved directly in x. The matrix coefficients in the rheology part are updated during the iteration to account for the extreme nonlinearities in Hibler's rheology. This means that bulk and shear viscosities are taken partly at the new time step. For consistency with the continuity equation, 9-point formulas are taken for the rheology. The formulation of the model ensures that the small diffusion coefficient A in Eqs. (69) to (71) is sufficient to provide computational stability.

g. *Technical differences between isopycnic and eulerian coordinates*

If the equation of motion is written in momentum-conserving flux form, ρv is predicted in z coordinates and ρvh in a layer model. The basic difference between both vertical representations is that the layer thickness is variable in a layer model. Consequently the pressure gradient term in the equation of motion is weighted with h in a layer model. The resulting equations are nonlinear. If the wave equation is derived in order to obtain an implicit formulation for the layer thickness h only, the resulting Eq. (93) is also nonlinear. In z coordinates the comparable equation is linear, except for a weak nonlinearity due to vertical density variations. Here, it is not appropriate to solve the nonlinear wave equation with a technique where the matrix coefficients are determined and the resulting matrix is inverted and kept fixed for a number of time steps as in Maier-Reimer and Hasselmann (1987). Because the matrix coefficients can change rapidly from time step to time step, the matrix has to be updated every time step. Furthermore, the nonlinearity in the pressure-gradient term is part of the geostrophic balance. If layer thicknesses vary slowly, it would be possible to use a method where the matrix coefficients are calculated once every time step. However, rapid changes in the layer thicknesses as a result of the mixed-layer dynamics mainly due to detrainment make it necessary to update the matrix coefficients at each iteration. Without this procedure strong imbalances in the geostrophy would excite inertia-gravity waves, which would contribute to an increased noise level in the model. Therefore, the matrix is updated after each iteration step. This allows a reduction of explicit diffusion of momentum for computational stability reasons, but it enhances the costs of running such a model. It should be noted that the enclosure of a mixed layer that is responsible for rapid layer-thickness changes is one reason for the complex numerical methods needed for finding the solution at each time step. The advantage, however, is that no stability restrictions appear, as the x direction is treated directly by linear equations. A spatial filter is not required here.

3. Conclusions

In this technical description the major conceptual problems to realizing an ocean general circulation model based on isopycnal coordinates have been investigated. They arise essentially through the nonlinear equation of state and the inclusion of salt as a dynamically active tracer. Alongisopycnal discretization errors of the advection formulation for temperature and salinity, denoted as artificial cabbeling as well as the physically existing cabbeling through mixing along an isopycnal cause a coordinate drift that has to be compensated. The proposed solution is to make use of the underdetermined nature of the set of equations by introducing constraints that select one solution out of the infinite number of basically allowed solutions. The constraint selects that model state whose coordinate interfaces coincide with isopycnals. This is introduced by an appropriate formulation of all vertical exchange processes, such as entrainment/detrainment and cross-isopycnal mixing and convection, and allows one to compensate for the weak coordinate drift induced by cabbeling. An alternative technique to treat vanishing layers has been developed, essentially to have a scheme that best fits with the strategy for solving the primitive equations. This has been realized by choosing the well-known semi-implicit technique and by combining it with a predictor–corrector scheme. This yields a numerically stable integration at large time steps and makes the model relatively insensitive to the poleward convergence of the spherical grid. This has been achieved mainly with direct methods to solve the wave equation, the advection and diffusion of momentum, of temperature, and of salinity in the zonal direction. In order to, at least, have the prospect to run the model in a global mode, a model for the sea ice has been included. The viscous-plastic rheology, therefore, has the task to make the model less sensitive, while being used for climate drift experiments in a coupled atmosphere–ocean–ice model. The development of the mixed-layer model has two goals. First, the ideal behavior of the major parts of the deep ocean cannot be assumed near the surface. The parameterization of the surface boundary layer acts as a mediator between the atmosphere and the deep ocean. Second, the underestimated variability commonly observed in coupled ocean–atmosphere models is, hopefully, improved by making the time scale of air–sea interaction also dependent on the mixed-layer thickness. These extensions have to be understood as investment in future applications of this model.

APPENDIX

Comments on Time Discretization

a. The predictor–corrector scheme

Coupling of the semi-implicit steps has been described in Oberhuber (1986). If $\boldsymbol{\Psi}$ is the mass flux ($\rho v h$), Φ the mass content (ρh), Θ the heat content ($\rho\theta h$), and Π the salt content ($\rho S h$), then the predictor step may be written symbolically:

$$\boldsymbol{\Psi}^{*n+1} - \frac{\Delta t}{2}\mathbf{G}_{\Psi}^{*n+1} = \boldsymbol{\Psi}^{n} + \frac{\Delta t}{2}\mathbf{G}_{\Psi}^{*n} + \Delta t\mathbf{F}_{\Psi}^{*n} \quad (99)$$

$$\Phi^{*n+1} - \frac{\Delta t}{2}G_{\Phi}^{*n+1} = \Phi^{n} + \frac{\Delta t}{2}G_{\Phi}^{*n} + \Delta t F_{\Phi}^{*n} \quad (100)$$

$$\Theta^{*n+1} - \frac{\Delta t}{2}G_{\Theta}^{*n+1} = \Theta^{n} + \frac{\Delta t}{2}G_{\Theta}^{*n} + \Delta t F_{\Theta}^{*n} \quad (101)$$

$$\Pi^{*n+1} - \frac{\Delta t}{2}G_{\Pi}^{*n+1} = \Pi^{n} + \frac{\Delta t}{2}G_{\Pi}^{*n} + \Delta t F_{\Pi}^{*n}. \quad (102)$$

All equations are discretized in time using an Euler scheme; G represents all those terms that are treated implicitly, and F those terms that are explicitly taken forward; All remaining terms are collected in F; $\boldsymbol{\Psi}^{*n+1}$, Φ^{*n+1}, Θ^{*n+1}, and Π^{*n+1} are first guesses for the new time level $n+1$. The entrainment and detrainment rate and the resulting changes in the mass fluxes are treated implicitly in the first correction step. The solution of the mixed layer part is obtained with a Newtonian method to find zeros of the resulting nonlinear equation. Because no spatial derivatives occur, the following equations can be solved pointwise:

$$\boldsymbol{\Psi}^{**n+1} - \frac{\Delta t}{2}\mathbf{G}_{\Psi}^{**n+1} = \boldsymbol{\Psi}^{*n+1} - \frac{\Delta t}{2}\mathbf{G}_{\Psi}^{**n} \quad (103)$$

$$\Phi^{**n+1} - \frac{\Delta t}{2}G_{\Phi}^{**n+1} = \Phi^{*n+1} - \frac{\Delta t}{2}G_{\Phi}^{**n} \quad (104)$$

$$\Theta^{**n+1} - \frac{\Delta t}{2}\mathbf{G}_{\Theta}^{**n+1} = \Theta^{*n+1} - \frac{\Delta t}{2}\mathbf{G}_{\Theta}^{**n} \quad (105)$$

$$\Pi^{**n+1} - \frac{\Delta t}{2}\mathbf{G}_{\Pi}^{**n+1} = \Pi^{*n+1} - \frac{\Delta t}{2}\mathbf{G}_{\Pi}^{**n}, \quad (106)$$

where $\boldsymbol{\Psi}^{**n+1}$, Φ^{**n+1}, Θ^{**n+1}, and Π^{**n+1} are the corrected guesses for the new time level $n+1$. Finally, the implicit part of the advection and diffusion of momentum is formulated by solving the resulting equation directly in x and iterating in y. The equation is

$$\boldsymbol{\Psi}^{***n+1} - \frac{\Delta t}{2}\mathbf{G}_{\Psi}^{***n+1} = \boldsymbol{\Psi}^{**n+1} - \frac{\Delta t}{2}\mathbf{G}_{\Psi}^{***n}, \quad (107)$$

Finally, $\boldsymbol{\Psi}^{***n+1}$, Φ^{**n+1}, Θ^{**n+1}, and Π^{**n+1} are taken as final values for the new time level $n+1$. From these quantities the physical quantities u, v, h, ρ, θ, S, T, and σ_θ are determined.

b. Separation of model variables into basic quantities

In order to split the momentum, mass, heat, and salt content into the associated velocities, density, temperature, and salinity variables the following identity is used, where a and b represent any pair of variables:

$$(ab)^{n+1} - (ab)^{n} = \frac{a^n + a^{n+1}}{2}(b^{n+1} - b^n) + \frac{b^n + b^{n+1}}{2}(a^{n+1} - a^n). \quad (108)$$

This relation enables the prediction of the basic quantities and at the same time solves the full flux form of the equations of motion. With Eq. (93) an example was given of how the total mass content is separated into the density and the layer thickness.

c. Wave properties of the model

An exciting aspect of the model numerics is the wave equation (93), used to determine the time development of the layer thickness. It allows the deduction of how Rossby waves propagate in this isopycnal model. For simplicity, the limiting case for a large time step Δt is considered [$\Delta t \gg (f+\zeta)^{-1}$]. In this case, the quadratic terms in (93), which represent the inertia–gravity waves, can be neglected. This means physically that the geostrophic adjustment appears instantaneously. Furthermore, if (93) is applied to a two-layer reduced gravity model and rewritten symbolically as an analytic equation, this yields a pure equation for the propagation of Rossby waves:

$$\frac{\partial h}{\partial t} = g'\frac{\partial}{\partial x}\frac{h}{\zeta+f}\frac{\partial h}{\partial y} - g'\frac{\partial}{\partial y}\frac{h}{\zeta+f}\frac{\partial h}{\partial x} + G. \quad (109)$$

This now clearly demonstrates the behavior of Rossby waves in layer models that conserve potential vorticity exactly. In regions of constant potential vorticity, Rossby waves do not propagate since both mixed derivatives cancel. This is true as long as the forcing function G is negligible. This means that no extensive mixing, convective processes, or wind forcing occurs so that these are free waves.

After linearizing Eq. (109) with respect to a constant $h_0/(f_0+\zeta_0)$ and ignoring ζ_0, it simplifies to

$$\frac{\partial h}{\partial t} = \frac{g' h_0 \beta}{f_0^2}\frac{\partial h}{\partial x} + G, \quad (110)$$

where $(g' h_0 \beta)/f_0^2$ is the phase velocity of a Rossby wave in this linear system. A comparable linearization is carried out to derive a QG model. Here the basic difference relative to this model is visible. Since changes of layer thickness associated with outcropping at the surface or vanishing at topographic boundaries or even

existing in the free ocean are strong compared with the variation of the Coriolis parameter f, Rossby waves propagate rather differently in this model compared with a QG model. This was one of the conclusions from an eddy-resolving experiment carried out by Bleck and Boudra (1986) with their isopycnic coordinate model.

d. Acceleration method

In addition to the implicit time step scheme an acceleration method was implemented. It follows the idea of Bryan (1984). It enables the achievement of a stationary state within a shorter integration time. In order to do this the momentum, temperature, and salinity equation is multiplied with some coefficient ω_k that depends only on the layer index. The equations are rewritten

$$\omega_k \frac{\partial}{\partial t}(\rho uh, \rho vh, \theta, S)_k = (J_{\rho uh}, J_{\rho vh}, J_\theta, J_S)_k. \quad (111)$$

Note that the continuity equation, which is a predictive equation for the coordinates, is not accelerated. Otherwise, the variable topography would introduce a strong barotropic mode as well as an unphysical coupling between vertical modes. The first layer is not accelerated, so that $\omega_1 = 1$. All acceleration coefficients ω_k for deeper layers are given by the relation between the phase speed of the kth and the phase speed of the first baroclinic mode of the internal gravity waves. Consequently, the acceleration method does not directly influence the mixed layer, and therefore it is possible (with some restrictions) to force the model with a seasonal cycle. Only the time development in deeper layers is directly influenced. The big advantage is that advection of heat and salt, which is responsible for the largest time scales in the deep ocean, is accelerated. The disadvantages of this method are the same as in other acceleration methods, namely that heat and salt are not conserved as long as the local changes in time do not vanish. In the stationary state, however, the calculated state is identical to the state that would be achieved with $\omega_k = 1$.

e. Code properties

The model development started on a Cyber173 and was continued on a Cyber205. Currently, the code is optimized for computers such as Cray-2S and Cray-YMP. The present version of the code, called OPYC (*O*cean iso*PYC*nal model), easily achieves 150 Mflops on a single processor of a Cray-YMP. Recently, sufficient parallelization for computers with shared memory is available, too. The code has been optimized so that it requires 12 CPU-seconds per day prediction with a 1-day time step for a global version formulated on a T42-Gaussian grid, which has $128 \times 64 \times 9$ grid points and requires about 5 MW of memory. Up to 5-day time steps are possible. The sea ice model runs at 170 Mflops for the example above and contributes with only 2%–3% to the total CPU time. Thus, the required resources are reasonable compared with the additional operations necessary to treat the time-dependent coordinates, mixed layer, and sea ice. The good performance is mainly achieved by applying "line-iteration" as a method to solve the implicit problems for waves, advection, and diffusion. The method offers a high degree of parallelism as well as the available long vectors necessary for a high optimization on a super computer and moderate memory consumption. The program language is standard FORTRAN77 with no extensions used. Therefore, the code can be ported even onto workstations such as SUN or IBM-RISC after using a preprocessor that converts the code for a scalar computer. Further utilities, such as the rotation of the spherical coordinates by Euler angles to avoid grid convergence at high latitudes or a multigrid method for a more efficient spin up of the model, can be used. Finally, a complete code package for postprocessing requires only the GKS routines for plotting. An extended version of the GRIB code (*Gri*dded *B*inary) developed by the WMO and ECMWF is used as postprocessing file format.

REFERENCES

Arakawa, A., 1966: Coputational design of long-term numerical integration of the equations of fluid motion. *J. Comput. Phys.*, **1**, 119–143.

——, 1972: Design of the UCLA general circulation model. *Numerical Simulation of Weather and Climate*, Tech. Rep. No. 7, Department of Meteorology, University of California, Los Angeles, 116 pp.

Berliand, M. E., and T. G. Berliand, 1952: Determining the net longwave radiation of the Earth with consideration of the effect of cloudiness. Isv. Akad. Nauk. SSSR Ser. Geofis, No. 1.

Berliand, T., 1960: Methods of climatological computation of total incoming solar radiation. *Meteor. Gidrol.*, **5**, 9–12. [MGA 12: 1486.]

Bleck, R., 1974: Short-range prediction in isentropic coordinates with filtered and unfiltered numerical models. *Mon. Wea. Rev.*, **102**, 813–929.

——, 1978: Finite-difference equations in generalized vertical coordinates. Part I: Total energy conservation. *Beitr. Phys. Atmos.*, **50**, 186–199.

——, 1979: Finite-difference equations in generalized vertical coordinates. Part II. Potential vorticity conservation. *Beitr. Phys. Atmos.*, **52**, 95–105.

——, 1984: An isentropic coordinate model suitable for lee cyclogenesis simulation. *Riv. Meteor. Austronaut.*, **43**, 189–194.

——, and D. B. Boudra, 1981: Initial testing of a numerical ocean circulation model using a hybrid (quasi-isopycnic) vertical coordinate. *J. Phys. Oceanogr.*, **11**, 755–770.

——, and ——, 1986: Wind-driven spin-up in eddy-resolving ocean models formulated in isopycnic and isobaric coordinates. *J. Geophys. Res.*, **91**, 7611–7621.

Bogue, N. M., R. X. Huang, and K. Bryan, 1986: Verification experiments with an isopycnic coordinate ocean model. *J. Phys. Oceanogr.*, **16**, 985–990.

Boris, J. P., and D. L. Book, 1973: Flux-corrected transport. I: SHASTA, a fluid transport algorithm that works. *J. Comput. Phys.*, **11**, 38–69.

Bryden, H., 1973: New polynomials for thermal expansion, adiabatic temperature gradient and potential temperature of sea water. *Deep-Sea Res.*, **20**, 401–408.

Bryan, K., 1969: A numerical method for the study of the circulation of the world ocean. *J. Comput. Phys.*, **4**, 347–376.
——, 1984: Accelerating the convergence to equilibrium of ocean-climate models. *J. Phys. Oceanogr.*, **14**, 666–673.
Budyko, M. I., 1974: *Climate and Life.* Academic Press, 508 pp.
Bunker, A. F., 1976: Computations of surface energy flux and annual air–sea interaction cycles of the North Atlantic Ocean. *Mon. Wea. Rev.*, **104**, 1122–1140.
Crowley, W. P., 1968: Numerical advection experiments. *Mon. Wea. Rev.*, **96**, 1–11.
Cox, M. D., 1975: A baroclinic numeric model of the world ocean: Preliminary results. Numerical Model Of Ocean Circulation. Natl. Acad. Sci., Washington, D.C., 107–120.
——, 1984: A primitive equation three-dimensional model of the ocean. GFDL Ocean Group Tech. Rep., No. 1, GFDL/NOAA, Princeton University, Princeton, 250pp.
Deardorff, J. W., 1983: A multi-limit mixed-layer entrainment formulation. *J. Phys. Oceanogr.*, **13**, 998–1002.
Denman, K. L., and M. Miyake, 1973: Upper-layer modification at Ocean Station Papa: Observations and simulations. *J. Phys. Oceanogr.*, **3**, 185–196.
Esbensen, S. K., and Y. Kushnir, 1981: The heat budget of the Global Ocean: An atlas based on estimates from surface marine observations. Available from Climate Research Institute, Oregon State University, Rep. No. 29, 27 pp.
Garwood, R. W., 1977: An oceanic mixed layer model capable of simulating cyclic states. *J. Phys. Oceanogr.*, **7**, 455–468.
——, Jr., P. C. Gallacher, and P. Müller, 1985a: Wind direction and equilibrium mixed layer depth: General theory. *J. Phys. Oceanogr.*, **15**, 1525–1531.
——, ——, and ——, 1985b: Wind direction and equilibrium mixed layer depth in the tropical Pacific Ocean. *J. Phys. Oceanogr.*, **15**, 1532–1538.
Gaspar, P., 1988: Modeling the seasonal cycle of the upper ocean. *J. Phys. Oceanogr.*, **18**, 161–180.
Haney, R. L., 1971: Surface thermal boundary conditions for the ocean circulation models. *J. Phys. Oceanogr.*, **1**, 241–248.
Hibler, W. D., III, 1979: A dynamic thermodynamic sea ice model. *J. Phys. Oceanogr.*, **9**, 815–846.
——, and K. Bryan, 1987: A diagnostic ice–ocean model. *J. Phys. Oceanogr.*, **17**, 987–1015.
Hsiung, J., 1985: Estimates of global oceanic meridional heat transport. *J. Phys. Oceanogr.*, **15**, 1405–1413.
——, 1986: Mean surface energy fluxes over the Global Ocean. *J. Geophys. Res.*, **91**, 10 585–10 606.
Huang, R. X., and K. Bryan, 1987: A multilayer model of the thermohaline and wind-driven circulation. *J. Phys. Oceanogr.*, **17**, 1909–1924.
Isemer, H.-J., and L. Hasse, 1987: *The BUNKER Climate Atlas of the North Atlantic Ocean.* Vol. 2: *Air–Sea Interactions.* Springer-Verlag, 256 pp.
Kraus, E. B., and J. S. Turner, 1967: A one-dimensional model of the seasonal thermocline. *Tellus*, **1**, 88–97.
Kwizak, M., and A. J. Robert, 1971: A semi-implicit scheme for a grid-point atmospheric model of the primitive equations. *Mon. Wea. Rev.*, **99**, 32–36.
Large, W. G., and S. Pond, 1981: Open ocean momentum measurements in moderate to strong winds. *J. Phys. Oceanogr.*, **11**, 324–336.
——, and ——, 1982: Sensible and latent heat flux measurements over the sea. *J. Phys. Oceanogr.*, **12**, 464–482.
Lemke, P., 1987: A coupled one-dimensional sea ice–ocean model. *J. Geophys. Res.*, **92**, 13 164–13 172.
Martin, P. J., 1985: Simulation of the mixed layer at OWS November and Papa with several models. *J. Geophys. Res.*, **90**, 903–916.
McDougal, T. J., and J. A. Church, 1986: Pitfalls with the numerical representation of isopycnal and diapycnal mixing. *J. Phys. Oceanogr.*, **16**, 196–199.
Maier-Reimer, E., and K. Hasselmann, 1987: Transport and storage of CO_2 in the ocean—An inorganic ocean-circulation carbon cycle model. *Climate Dyn.*, **2**, 63–90.
Niiler, P. P., 1975: Deepening of the wind-mixed layer. *J. Mar. Res.*, **33**, 405–422.
——, and E. B. Kraus, 1977: One-dimensional model of the seasonal thermocline. *The Sea*, Vol. VI, Wiley–Interscience, 97–115.
Oberhuber, J. M., 1986: About some numerical methods used in an ocean general circulation model with isopycnic coordinates. *Advanced Physical Oceanographic Numerical Modelling, Series C: Mathematical and Physical Sciences*, J. J. O'Brien, Ed., NATO ASI Series, Vol. 186, 511–522.
——, 1988: An atlas based on the "COADS" data set: The budgets of heat, buoyancy and turbulent kinetic energy at the surface of the global ocean. Max-Planck-Institute for Meteorology, Rep. 15, 199 pp.
Paltridge, G. W., and C. M. R. Platt, 1976: *Radiative Processes in Meteorology and Climatology.* Elsevier, 53–66 pp.
Parkinson, C. L., and W. M. Washington, 1979: A large-scale numerical model of sea ice. *J. Geophys. Res.*, **84**, 311–337.
Paulson, C. A., and J. J. Simpson, 1977: Irradiance measurements in the upper ocean. *J. Phys. Oceanogr.*, **7**, 952–956.
Redi, M. H., 1982: Oceanic isopycnal mixing coordinate rotation. *J. Phys. Oceanogr.*, **12**, 1154–1158.
Reed, R. K., 1977: On estimating insolation over the ocean. *J. Phys. Oceanogr.*, **7**, 482–485.
Robinson, A. R., 1965: A three-dimensional model of inertial currents in a variable-density ocean. *J. Fluid Mech.*, **21**, 211–223.
Schopf, P. S., 1983: On equatorial waves and El Niño. I: Effects of air–sea thermal coupling. *J. Phys. Oceanogr.*, **13**, 1878–1892.
——, and M. A. Cane, 1983: On equatorial dynamics, mixed layer physics and sea surface temperature. *J. Phys. Oceanogr.*, **13**, 917–935.
——, and D. E. Harrison, 1983: On equatorial waves and El Niño. I: Influence of initial states on wave-induced currents and warming. *J. Phys. Oceanogr.*, **13**, 936–948.
Seckel, G. R., and F. H. Beaudry, 1973: The radiation from sun and sky over the North Pacific Ocean (Abstract), *Trans. Amer. Geophys. Union*, **54**, 1114.
Semtner, A. J., 1974: An oceanic general circulation model with bottom topography. Numerical simulation of weather and climate, Department of Meteorology, University of California, Los Angeles, Tech. Rep. No. 9, 99 pp.
——, 1986: Finite-Difference Formulation of a World Ocean Model. Advanced Physical Oceanographic Numerical Modelling. J. J. O'Brien, Ed., NATO ASI Series, Series C: Mathematical and Physical Sciences, Vol. 186, 187–202.
Shapiro, M. A., 1975: Simulation of upper-level frontogenesis with a 20-level isentropic coordinate primitive-equation model. *Mon. Wea. Rev.*, **103**, 591–604.
Smagorinsky, J. S., 1963: General circulation experiments with the primitive equations. I: The basic experiment. *Mon. Wea. Rev.*, **91**, 99–164.
Smolarkiewicz, P. K., 1982: The multidimensional Crowley Advection Scheme. *Mon. Wea. Rev.*, **110**, 1968–1983.
UNESCO, 1981: The Practical Salinity Scale 1978 and the International Equation of State of Seawater 1980. (UNESCO Tech. Paper.) *Mar. Sci.*, No. **36**, 13–21.
Weare, B. C., P. T. Strub, and M. D. Samuel, 1981: Annual mean surface heat fluxes in the tropical Pacific Ocean. *J. Phys. Oceanogr.*, **11**, 705–717.
Woodruff, S. D., R. J. Slutz, R. L. Jenne, and P. M. Steurer, 1987: A Comprehensive Ocean–Atmosphere Data Set. *Bull. Amer. Meteor. Soc.*, **68**, 1239–1250.
Wright, P., 1988: An Atlas based on the "COADS" data set: Fields of mean wind, cloudiness and humidity at the surface of the global ocean. Max-Planck-Institute for Meteorology Rep. 14, 70 pp.
Zalesak, S. T., 1979: Fully multidimensional flux-corrected transport algorithms for fluids. *J. Comput. Phys.*, **31**, 335–362.
Zillmann, J. W., 1972: A study of some aspects of the radiation and the heat budgets of the Southern Hemisphere oceans. Bur. of Meteorol., Dep. of the Interior, Canberra, Australia, *Meteor. Stud.*, **26**, 562 pp.